EXAMINATION OF TISSUE TEMPERATURE PROFILE DURING PHOTOTHERMAL INTERACTION OF LASER IRRADIATION

by

Muhammed Hakan Köseoğlu

B.S., Electronics Engineering, Erciyes University, 2003

Submitted to the Institute of Biomedical Engineering
in partial fulfillment of the requirements
for the degree of
Master of Science
in
Biomedical Engineering

Boğaziçi University
September 2007

ACKNOWLEDGEMENTS

I would like to thank to my supervisor Assist. Prof. Murat Gülsoy for giving me the opportunity to work on this topic, his kind academic support and his ability about looking at events from different points of view that contributes me for exceeding difficulties during the time of this study.

I would like to thank Prof. Dr. İnci Çilesiz, İstanbul Technical University, for being a member of my thesis committee, and lending the 980-nm diode laser source.

I would like to thank Assist. Prof. Ata Akın for being a member of my thesis committee.

And my friends. I would like to give my special thanks to research assistants Haşim Özgür Tabakoğlu, Özgüncem Bozkulak and Ertuğrul Burteçin Aksel. I am very grateful for your patience, kind friendship and academic supports. Thank you my friends.

Şahide Köseoğlu and Nureddin Köseoğlu, my lovely family. This thesis dedicated to you.

ABSTRACT

EXAMINATION OF TISSUE TEMPERATURE PROFILE DURING PHOTOTHERMAL INTERACTION OF LASER IRRADIATION

During laser surgery, temperature measurement is critical in order to know the photothermal effect of laser irradiation on tissue. Depending on the duration and peak value of the temperature achieved, different tissue responses take place such as coagulation, vaporization, melting and carbonization. There are extensive studies about photothermal effects of laser tissue interaction. In all these studies, measuring temperature accurately is the essential part. Different methods are available for measuring tissue temperature resulting from absorption of laser energy. For deep measurement, temperature sensing probes are the most commonly used devices in biomedical applications. In this study, the temperature values at different radial and axial distances were measured during laser (980–nm diode laser) irradiation from different types of tissues (lamb kidney, heart and brain). Moreover, the effects of different power levels (2W, 3W, 4W) and different distances from target point on tissue temperature changes were compared. Thermocouple was used as temperature measuring device during laser irradiation. The deviations in the measurement of direct absorption of laser energy by thermocouple needles were taken into account. As a result of the experiments, it was observed that temperature increases are linearly positively correlated with the laser power levels and, the temperature decreases exponentially as the distance from the target point of laser light increases.

Keywords: Laser-tissue interaction, 980-nm diode laser, photo-thermal effect, thermocouple

ÖZET

LASER DOKU ETKİLEŞİMİ ESNASINDA DOKUDAKİ SICAKLIK PROFİLİNİN İNCELENMESİ

Laser uygulamalarında oluşan sıcaklık artışının bilinmesi, dokudaki etkiyi tayin etmek için kritik bir öneme sahiptir. Elde edilen farklı sıcaklık değerlerine ve sürelerine bağlı olarak koagülasyon, buharlaşma, karbonizasyon ve erime gibi değişik etkiler görülür. Laser doku etkileşiminin ısısal boyutu ile ilgili birçok çalışma mevcuttur. Bütün bu çalışmalarda esas olan şey, doğru sıcaklık değerlerinin ölçülmesidir. Laser ışığının soğrulması sonucu dokuda oluşan sıcaklık değerlerinin ölçülmesinde birçok metot mevcuttur. Bu metotlar içerisinde sıcaklık algılayıcı problar biyomedikal uygulamalarda derinlemesine (doku içi) ölçümlerde en sık kullanılan tekniktir. Bu çalışmada, değişik dokuların (kuzu beyni, böbreği ve kalbi) 980-nm diyot laser uygulamasına maruz kalması durumunda, dokulardaki derinlemesine değişik mesafelerdeki sıcaklık artışları gözlemlenmiştir. Laser çıkış güç seviyelerinin ve laser hedef noktasına olan uzaklığın sıcaklık artışına etkisi karşılaştırılmıştır. Sıcaklık ölçmek amacıyla ısılçiftler kullanılmıştır. Isılçift problarının laser ışığını doğrudan soğurması sonucu ölçümlerde oluşabilecek yanılgı payı göz önünde bulundurulmuştur. Deneylerin sonucunda; laser çıkış gücüyle sıcaklık artışının doğru orantılı bir şekilde değiştiği ve laser hedef noktasından uzaklaşıldıkça dokuda ölçülen sıcaklık artışının üssel olarak azaldığı gözlemlenmiştir.

Anahtar Sözcükler: Laser-doku etkileşimi, 980-nm diyot laser, foto-termal etkileşim, ısılçift

TABLE OF CONTENTS

LIST OF FIGURES

LIST OF TABLES

LIST OF SYMBOLS

ºC	Degree Celsius
g	Gram
s	Second
ms	Millisecond
mA	Milliampere
mm	Millimeter
µm	Micrometer
nm	Nanometer
W	Watt

LIST OF ABBREVIATIONS

AC	Alternating Current
ArF	Argon Fluoride
ArI	Argon Iodide
CO_2	Carbon dioxide
CW	Continuous Wave
DC	Direct Current
EMF	Electro motor force
Er:YAG	Erbium Yttrium Aluminum Garnet
He	Helium
Ho:YAG	Holmium Yttrium Aluminum Garnet
HpD	Hematoporphyrin derivative
IR	Infrared
LASER	Light Amplification by the Stimulated Emission of Radiation
LED	Light Emitting Diode
LITT	Laser-induced interstitial thermotherapy
Nd:YAG	Neodymium Yttrium Aluminum Garnet
Ne	Neon
NiAl	Nickel Aluminide
NiCr	Nickel Chromium
NIR	Near Infrared
RTO	Resistive temperature detectors
PDT	Photodynamic therapy
PTFE	Poly Tetra Fluoro Ethylene
PVC	Poly Vinyl Chloride
UV	Ultraviolet
XeCl	Xenon Chloride

1. INTRODUCTION

1.1 Motivation and Objectives

Lasers have been used widely in almost all medical fields. Neurosurgery and cardiovascular applications are some of the popular areas where lasers are being used. In these applications, different interaction types (photochemical, photothermal, photoablation, plasma-induced ablation and photodisruption), which occur depending on exposure times, power density and optical properties of the tissue, are being used related to different intentions. Photothermal interaction is one of the most widely used interaction types in medical applications [1,2].

At photothermal interaction, light energy is converted to heat energy. This transformation occurs as a result of the absorption of light by the main chromophores (water or hemoglobin) of the tissue and then the increase in vibration. Light in near infrared and infrared region is highly absorbed by water. Diode lasers (range from 800-nm to 1000-nm), Nd:YAG laser, Er:YAG laser and CO_2 laser operate in this region of the spectra [3].

Diode lasers have advantages in terms of being practical and economical. Among those diode lasers, 980-nm diode laser has a special characteristic that one of the peaks in absorption spectra of water stands out at this wavelength.

Thermal interactions are obtained by continuous or pulsed laser light. Depending on the duration and peak value of the temperature, different interactions like hyperthermia, coagulation, vaporization, melting and carbonization are acquired [3].

There are extensive clinical applications where photothermal interactions of laser irradiation are being used. The crucial point in these applications is to know the temperature values at different radial and axial distances from the target point of tissue.

Many methods are available for measuring temperature changes in tissue resulting from the absorption of laser energy. Because of their tough designs, simplicity in operation and capability of measuring temperature at a point, electrical probes (especially thermocouples) are the most commonly used devices to examine tissue temperature profile during laser irradiation. Although the measured temperatures increase because of the direct absorption of laser energy by thermocouple needle, there are many areas (real time temperature monitoring during interstitial laser heating of tumors, laser angioplasty etc.) where thermocouples are used widely as the temperature sensing device [2].

The goal of this project is to measure the temperature values at different radial and axial distances during laser irradiation from different types of tissues. According to obtained results, optimum parameters will be determined to minimize thermal damage to the neighborhood of target tissue.

The effect of different power levels on different type of tissues (lamb brain, heart, and kidney) will be tested *in vitro* by using 980-nm diode laser and tried to make a relation between power levels, measured temperature and photothermal effect.

1.2 Outline

In chapter 2, theory of laser, medical use of laser, laser tissue interaction, photothermal interaction and thermocouple are explained.

Chapter 3 gives detailed information about materials and methods used in this study. Laser system, tissue preparation, temperature measurement system and experimental setups for deep measurements are stated in this chapter.

The results of 3-mm and 5-mm deep measurements are demonstrated in Chapter 4. The effects of distances from the target point and different-power lasers on tissue temperature increment are shown on graphs and made a comparison according to the different tissue samples. In addition to these graphs, three dimensional plotting of the

temperature increments depending on time and distances are given by using *MATLAB* and *surf* command.

In chapter 5, a general conclusion and contribution of this study for further scientific works can be found.

2.THEORY

2.1 Theory of Laser

Laser is an acronym of Light Amplification by the Stimulated Emission of Radiation. The full name itself indicates the major processes involved in laser production.

Laser is basically produced by the stimulated emission mechanism. It consists of a flash lamp, a laser medium and two mirrors (Figure 2.1). First, the flash lamp injects light into the laser medium, stimulating atoms in it and exciting the electrons at the outermost layer of the atoms. At this moment, some electrons will return to a lower energy level by emitting photons. The emitted photons will be reflected by the mirrors set at the two ends of the laser medium to stimulate more electrons to undergo stimulated emissions, thus increasing the intensity of the laser. One of the mirrors at the two ends will reflect all the photons while the other will reflect most of them, and the remaining small portion of photons that passes through the latter mirror constitute the laser we see [4].

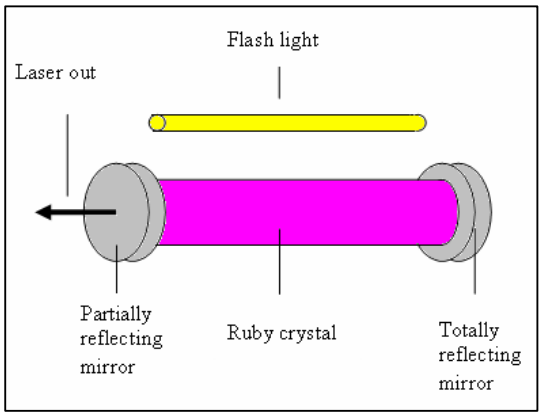

Figure 2.1 Simplified structure of a ruby laser [5].

The laser produced from stimulated emission has the following three major characteristics

- It is monochromatic. Only light of a single wavelength is produced in the whole process. This differs from ordinary light such as sunshine or lamplight, which is composed of different wavelengths of light, being close to white light.
- It is coherent. All photons have the same phase and the same polarization, hence they produce a very high intensity when they superpose. The lights we see in daily life have random phases and polarization, and hence they are relatively much weaker.
- It has a very narrow and collimated ray, and hence it is very powerful. In contrast, lamplight diverges towards different directions and has a low intensity [1, 4].

The laser medium can be solid, liquid, or gas and the pump source can be an electrical discharge, a flash lamp, or another laser. The specific components of a laser vary depending on the laser medium and whether the laser is operated continuously (cw) or pulsed.

Lasers can be classified according to their medium properties. Gas lasers (Excimer, Nitrogen, He-Ne, ArI, CO_2), solid-state lasers (Nd:YAG, Ho:YAG, Er:YAG), dye lasers and diode lasers are the typical laser types. In these laser types, diode lasers have advantages in terms of being practical and economical.

A laser diode is formed by doping a very thin layer on the surface of a crystal wafer. The crystal is doped to produce an n-type region and a p-type region to obtain a p-n junction. Simplified structure of a diode laser is shown in Figure 2.2.

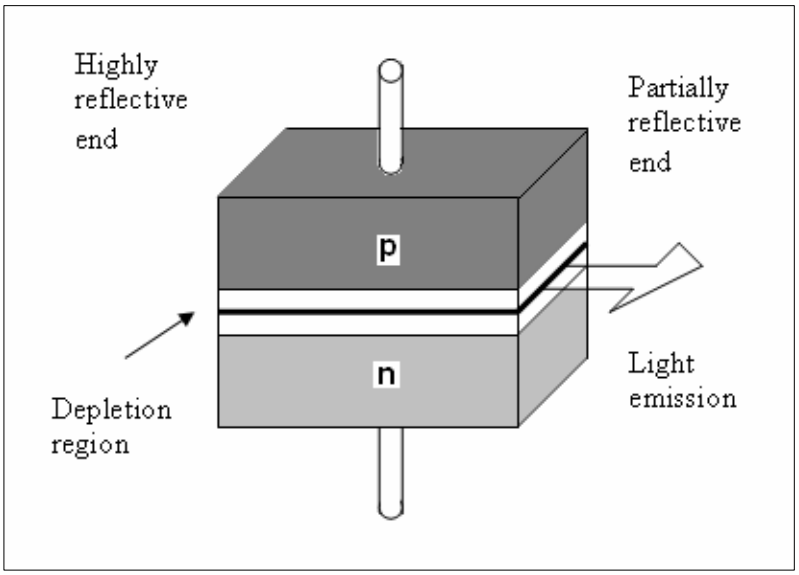

Figure 2.2 Simplified structure of a diode laser [6].

When this structure is forward biased, holes from the p-region are injected into the n-region, where electrons are the majority carrier. Similarly, electrons from the n-region are injected into the p-region, where holes are the majority carrier. When an electron and a hole are present in the same region, they may recombine by spontaneous emission. That is, the electron may re-occupy the energy state of the hole, emitting a photon with energy equal to the difference between the electron and hole states involved. These injected electrons and holes represent the injection current of the diode, and spontaneous emission gives the laser diode below lasing threshold similar properties to an LED. Spontaneous emission is necessary to initiate laser oscillation, but it is a source of inefficiency once the laser is oscillating.

Under suitable conditions, the electron and the hole may coexist in the same area for quite some time before they recombine. Then a nearby photon with energy equal to the recombination energy can cause recombination by stimulated emission. This generates another photon of the same frequency, traveling in the same direction, with the same polarization and phase as the first photon. This means that stimulated emission causes gain

in an optical wave in the injection region, and the gain increases as the number of electrons and holes injected across the junction increases.

The gain region is surrounded with an optical cavity to form a laser. The two ends of the crystal are cleaved to form perfectly smooth, parallel edges, forming a Fabry-Perot resonator. Photons emitted into a mode of the waveguide will travel along the waveguide and be reflected several times from each end face before they are emitted. As a light wave passes through the cavity, it is amplified by stimulated emission, but light is also lost due to absorption and by incomplete reflection from the end facets. Finally, if there is more amplification than loss, the diode begins to "lase" [7].

2.2 Lasers in Medicine

Lasers are widely used in almost all medical fields. First, they were used in ophthalmology, since the eye and its interior belong to the easiest accessible organs because of its high transparency. Dentistry was the second clinical discipline to which lasers were introduced. The major effort of clinical laser research is focusing on various kinds of tumor treatments such as photodynamic therapy (PDT) and laser-induced interstitial thermotherapy (LITT). These play significant role in many other medical disciplines like gynecology, urology, and neurology [8,9,10].

In 1960s laser biophysics outlined light-tissue and light-substance interactions. Photodynamic Therapy (PDT) that is directly related with light tissue and light substance interaction has become one of the major treatments of cancer. A photosensitizer hematoporphyrin derivative (HpD) is employed as substance, which accumulates into cancerous cells. After a certain period of time, laser irradiation is applied and photosensitizers are activated. Highly toxic compounds are released by decaying of choromophores. This event causes some cell structures to be oxidized and eventually cell death.

Laser-Induced Interstitial Thermotherapy (LITT) is another method also used for tumor removal. LITT removes tissue by heat effect and coagulate surrounding. Due to the associated coagulation of blood vessels, severe hemorrhages are less likely to occur that in conventional surgery. This is of particular importance in the case of tumors because they are usually highly vascularized [8].

Biostimulation is another important medical application of lasers. Laser have been used to treat skin problems (hair growth and wound healing), to introduce and suppress cell proliferation (stimulated collagen synthesis, suppressed collagen synthesis), and for pain relief [3].

Angioplasty and cardiology, dermatology, orthopedics, and gastroenterology are the other medical areas of lasers that successful laser treatments have been reported. Laser medicine is not restricted to one or a few disciplines. It has meanwhile been introduced to almost all of them, and it is expected that additional clinical applications will be developed in the near future [11].

2.3 Laser Tissue Interaction

When the laser beam interacts with tissue, some different interaction types occur. A map of laser-tissue interaction types is shown in Figure 2.3. The interaction types can be classified as photochemical interactions, photothermal interactions, photoablation, plasma-induced ablation and photodisruption.

In Figure 2.3, the cycles give only a rough estimate of the associated laser parameters.

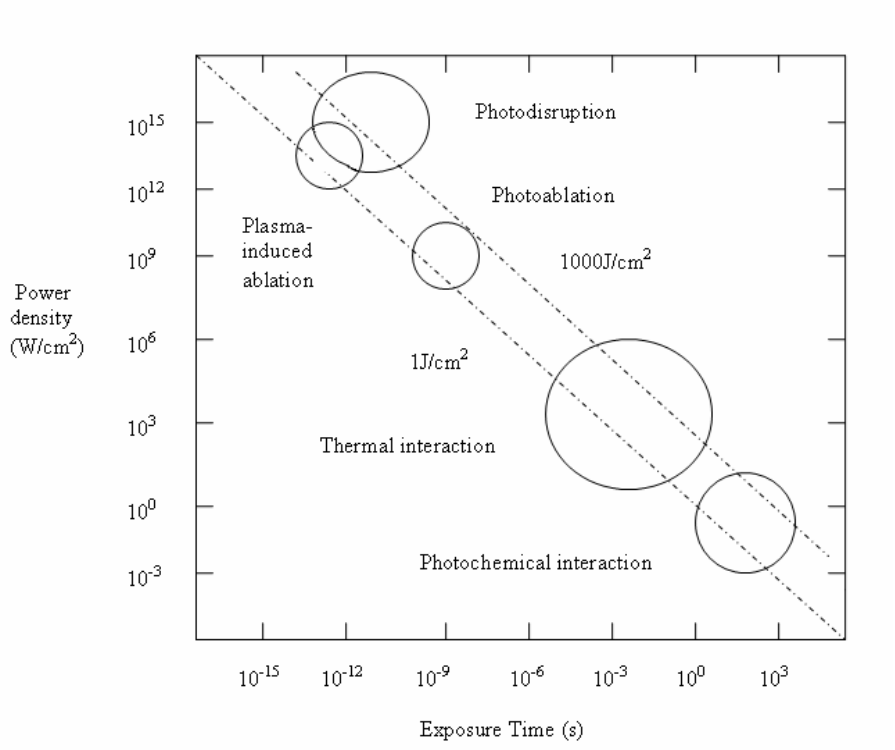

Figure 2.3 Map of laser tissue interactions [3].

The interaction of a laser light with tissue depends on exposure time, the wavelength of radiation itself, as well as the optical properties of the tissue (water content, blood circulation, heat conductivity, heat capacity, density of tissue) [3].

Despite the structural complexities, tissues can be regarded as homogeneous and isotropic mediums in which the propagation of the light radiation is described via basic optical phenomena like reflection, absorption, transmission and diffusion (Figure 2.4).

The group of photochemical interactions stems from empirical observations that light can induce chemical effects and reactions within macromolecules or tissue. Photochemical interactions take place at very low power densities (typically 1 W/cm^2) and long exposure times ranging from seconds to continuous wave. Careful selection of laser parameters yields a radiation distribution inside the tissue that is determined by scattering.

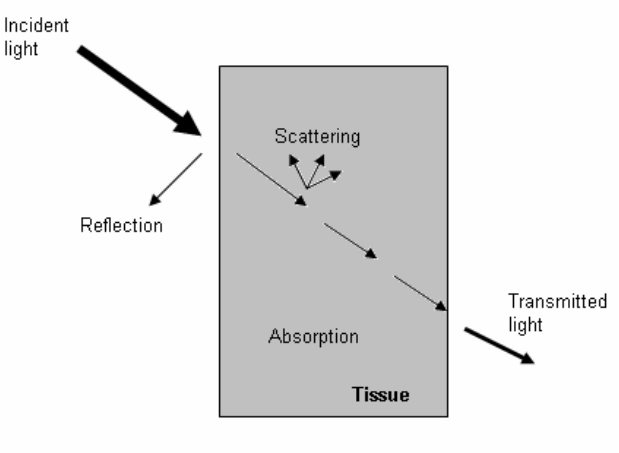

Figure 2.4 Diagram of the optical phenomena that take place during the interaction between light radiation and tissue**.**

In the field of medical laser physics, photochemical interactions mechanism plays a significant role during photodynamic therapy (PDT). Frequently, biostimulation is also attributed to photochemical interactions, although this is not scientifically ascertained [1,3].

Photoablation was identified as ablative photodecomposition, meaning that material is decomposed when exposed to high intense laser irradiation. Typical threshold values of this type of interaction are 10^7 – 10^8 W/cm^2 at laser pulse durations in the nanosecond range. The ablation depth is determined by the pulse energy up to a certain saturation limit. The main advantages of this ablation technique lie in the precision of etching process, its excellent predictability, and the lack of thermal damage to adjacent tissue [3]. Ultraviolet light-tissue interaction causes photoablation and is limited to this wavelength because of its high-energized photons.

Plasma-induced ablation and photodistruption mechanisms are very similar because both of these methods induce optical breakdown in tissue. The application of shorter high power laser pulses (10^{10} W/cm^2 for nanosecond pulses and 10^{12} W/cm^2 for picoseconds pulses) creates power densities, which generate such powerful electric fields that spontaneous ionization to free electrons and ionized atoms (plasma) is induced. After a certain degree of ionization has been reached, a rise in temperature of plasma follows. The

plasma then undergoes a sudden expansion accompanied by mechanical acoustic shockwave. The shockwave disrupts the tissue structure (photodistruption) [9].

A large part of surgical and clinical applications with laser is based on the conversion of optical radiation into thermal energy [8,12,13,14]. Photothermal interaction will be described detail at next section.

2.4 Photothermal Interactions

Photothermal interactions result from the transformation of absorbed light energy to heat energy. At this type of interaction a local temperature increase occurs. Thermal effects can be caused by either continuous wave (CW) or pulsed laser radiation. Photothermal effects are intervened primarily by absorption of optical energy and secondly governed by fundamental principles of heat transport. Depending on the duration and peak value of the temperature achieved, different effects like coagulation, vaporization, melting or carbonization may be distinguished. Photothermal effects of laser exposure can be seen in Figure 2.5.

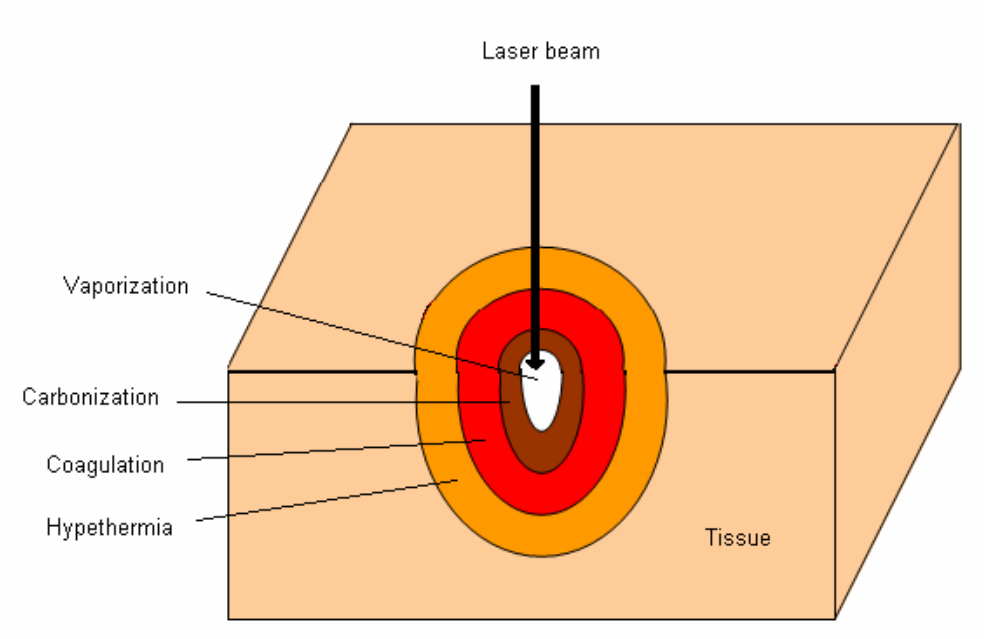

Figure 2.5 Photothermal effects of laser exposure

Thermal effects have their origin in bulk absorption occurring in molecular vibration rotation bands followed by a non radioactive decay. The reaction with a target molecule A can be considered as a two-steps process. First, absorption of a photon with an energy "hv" promotes the molecule to an excited state A^* ; and second, inelastic collisions with some partner M of the surrounding medium lead to a deactivation of A^* and a simultaneous increase in the kinetic energy of M. Therefore the temperature rise microscopically originates from the transfer of photon energy to kinetic energy. The two-steps process can be written as;

Absorption :$A+hv \rightarrow A^*$

Deactivation :$A^*+M(E_{kin}) \rightarrow A+M(E_{kin}+\Delta E_{kin})$

These two steps must be considered separately. First, absorption is facilitated due to the extremely large number of accessible vibrational states of most biomolecules. Second, the channels available for deactivation and thermal decay are also numerous, because typical energies of laser photons (Er:YAG laser: 0.35eV, Nd:YAG laser: 1.2eV, ArF laser: 6.4eV) exceed by far the kinetic energy of a molecule at room temperature which is only about 0.025eV. Thus, both of these steps are highly efficient provide the duration of laser exposure is properly selected [3].

The spatial extent and degree of tissue damage primarily depend on magnitude, exposure time, and placement of deposited heat inside the tissue. The deposition of laser energy, however, is not only a function of laser parameters such as wavelength, power density, exposure time, spot size, and repetition rate. It also strongly depends on optical tissue properties like absorption and scattering coefficients. For the description of storage and transfer of heat, thermal tissue properties are of primary importance such as heat capacity and thermal conductivity.

In biological tissue, absorption is mainly due to the presence of free water molecules, proteins, pigments, and other macromolecules. The absorption coefficient strongly depends on the wavelength of the incident laser radiation. In thermal interactions, absorption by water molecules plays a significant role. The absorption spectrum of water is shown in Figure 2.6. In the visible range, the absorption coefficient of water is extremely

small. Toward the IR range of the spectrum, however, water molecules are the dominant absorbers, since their absorption coefficient increases by several orders of magnitude.

In this study, 980-nm diode laser was used as the light source. As shown in Figure 2.6**,** one of the peaks in absorption spectra of water stands out at 980-nm.

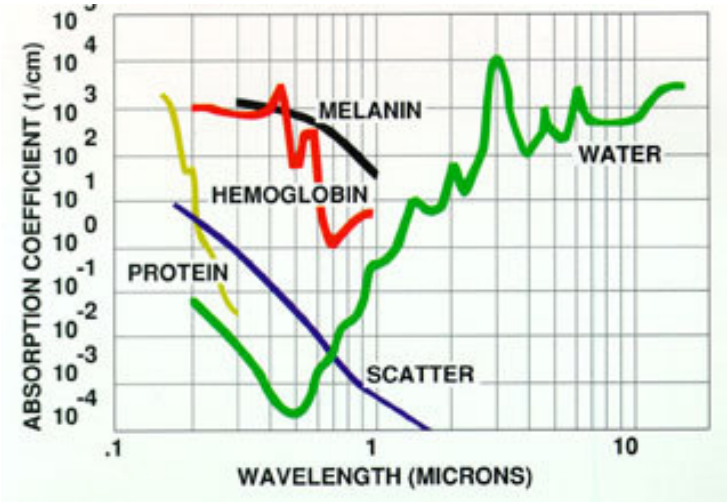

(a)

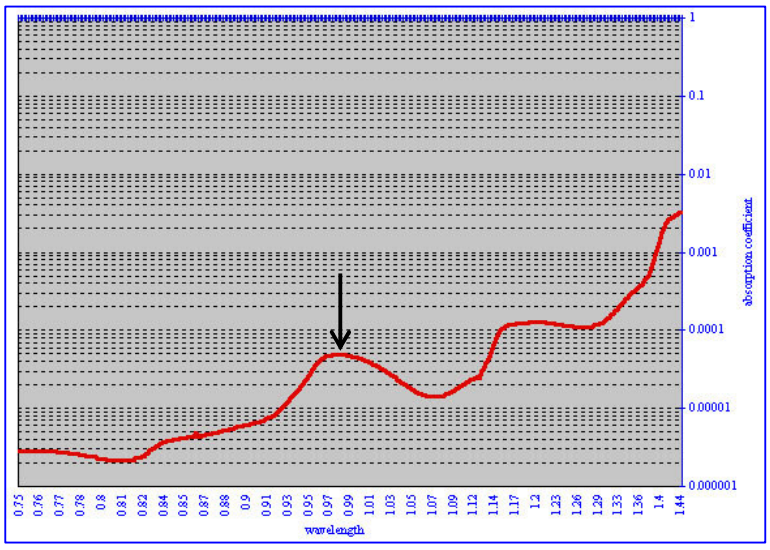

(b)

Figure 2.6. (a) Absorption spectrum of 4 main chromophores in tissues (water, hemoglobin, melanin and protein) [1], (b) One of the peaks in absorption spectra of water (980-nm) [9].

The biological effects of the photothermal type can be classified according to different thermodynamic processes to which the main histological modifications are summarized [Table 2.1].

Table 2.1
Histological modifications induced by the photothermal processes [9].

Temperature	**Histological Modifications**
43-45ºC	Conformational changes, shrinkage, hyperthermia (cell death)
50ºC	Reduction of enzymatic activity, cell immobility
60ºC	Denaturation of the proteins and collagen, coagulation
80ºC	Permeabilization of membranes
100ºC	Formation of extra cellular vacuoles and vaporization
>100ºC	Breaking of the vacuoles and carbonization
300-1000ºC	Thermoablation of the tissue
3350ºC	Vaporization of the carbon

Assuming a body temperature of 37°C, no measurable effects are observed for the next 5°C above this. The first mechanism by which tissue is thermally affected can be attributed to conformational changes of molecules. These effects are summarized in the single term hyperthermia ranging from 43°C-45°C. Beyond 50°C, a measurable reduction in enzyme activity is observed, resulting in a reduced energy transfer within the cell and immobility of the cell. Furthermore, certain repair mechanisms of the cell are disabled. Thereby, the fraction of surviving cells is further reduced.

At 60°C, denaturation of proteins and collagen occurs which leads to coagulation of tissue and necrosis of cells. Several treatment techniques (LITT etc) aim at temperatures just above 60°C. At even higher temperatures (>80°C), the membrane permeability is drastically increased, thereby destroying the otherwise maintained equilibrium of chemical concentrations.

At 100°C, water molecules contained in most tissues start to vaporize. The large vaporization heat of water is advantageous, because the vapor generated carries away

excess heat and helps to prevent any further increase in the temperature of adjacent tissue. Due to the large increase in volume during this phase transition, gas bubbles are formed including mechanical ruptures and thermal decomposition of tissue fragments.

Only if all water molecules have been vaporized, and laser exposure is still continuing, does the increase in temperature proceed. At the temperatures exceeding 150°C, carbonization takes place. To avoid carbonization, the tissue is usually cooled by either water or gas. Finally, beyond 300°C, melting can occur, depending on the target material [3].

As stated above, different biological effects occur depending on the temperature values change. Thus, during a laser application, measuring temperature value is significant in order to know its effect on tissue.

Many methods are available for measuring tissue temperature changes in tissue resulting from absorption of laser energy [2]. Most of the methods currently in use were developed originally for industrial applications and then adapted to biomedical applications such as vascular imaging, tumor imaging and hyperthermia monitoring [15, 16].

Four general methods of thermal monitoring can be identified: thermography, electrical probes, optical fiber probes and radiological imaging. Generally thermography and radiological imaging methods offer the advantages of noninvasiveness and multidimensionality, but at the expense of accuracy and spatial resolution. In biomedical laser applications, most temperature measurements are made using electrical probes or thermography, although increasing use of optical fiber probes might be anticipated [2].

Electrical probes for measuring tissue temperatures are implanted rather than applied externally. The four most common electrical temperature transducers are thermocouple, thermistors, resistive temperature detectors (RTOs) and integrated circuit sensors. RTOs are the most accurate and stable, but are expensive and seldom used clinically.

In this study, thermocouples were used to measure tissue temperature because of their tough designs, simplicity in operation and capability of measuring temperature at a point. The effects of direct absorption by thermocouple needles on the tissue temperature were taken into account.

2.5 Thermocouple

Thermocouples are the most commonly used temperature sensing devices. They can be made in very tough designs; they are very simple in operation and measure temperature at a point. Over different types they cover from -250°C to +2500°C.

The principal of operation is on the Seebeck effect. A temperature gradient along a conductor creates an EMF. If two conductors of different materials are joined at one point, an EMF is created between the open ends which are dependent upon the temperature of the junction. The junction is placed in the process; the other end (for the purposes of a standard output) is in iced water at 0^{o}C. This is called the reference junction. In the field the reference junction is usually at ambient temperature in the indicating unit and a cold junction compensation allowance is made. This is usually done through the indicator electronics. Provided that set temperature limits are not exceeded, inexpensive compensating wires can replace thermocouple conductors for part of the circuit. They replicate the thermoelectric performance of the thermocouple wires up to a certain temperature. Temperatures along the wires will not affect output voltage, providing that the alloys are thermocouple wire or compensating cable. Alloy combinations are chosen which produce a high EMF, are stable at temperature and readily available [2].

Thermocouple output depends on the alloy mix of the conductors. No two mixes will be identical and sensor calibration is required if high accuracy is needed. The performance of an individual sensor will drift with high temperature exposure. Lower temperature combinations are often called Base Metal.

The most common one is Type K NiCr v NiAl. These are limited to 1100^0C if any lifetime is expected. Above this temperature rare metals are used. Type R, Pt v PtRh(13%) is very common. These are much more expensive but can record up to 1700^0C (Type B) and remain stable for a reasonable lifetime.

A thermocouple consists of two conductors, welded together at the measuring point and insulated from each other long the length. It will usually have an outer protection sheath. PVC, Silicon rubber or PTFE insulators are common to 250^0C, above this Glass fiber or ceramic is used. The protection sheath is often a metal alloy which is inert to a particular process. At high temperatures ceramic sheaths are used.

The most common bimetallic combinations are summarized in Table 2.2. Each of these has a nonlinear temperature vs. voltage characteristics (Figure 2.7) that is usually fitted by a high order polynomial over a wide temperature ranger or a low order polynomial over a narrow temperature range.

Table 2.2
Common thermocouple metal combinations [2].

Type	+Metal	-Metal
E	Chromel	Constantan
J	Iron	Constantan
K	Chromel	Alumel
R	Platinum-13%Rhodium	Platinum
S	Platinum-13%Rhodium	Platinum
T	Copper	Constantan

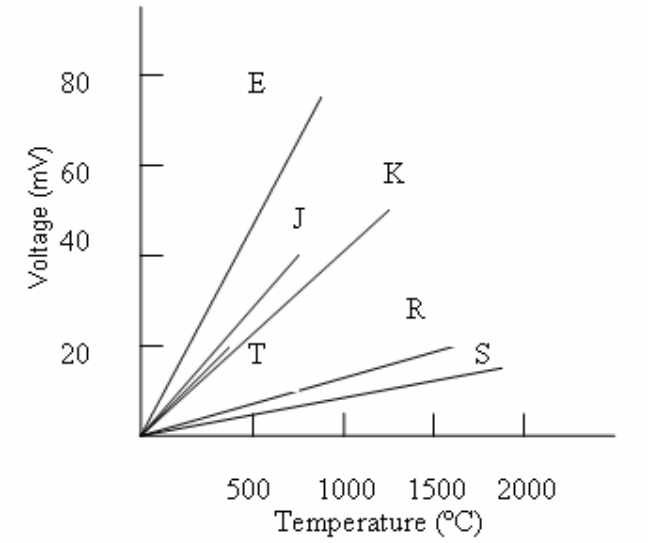

Figure 2.7 Temperature vs. voltage characteristic for six common thermocouple combinations [2].

In the biomedical laser field, thermocouples are the most often used for real-time temperature monitoring during interstitial laser heating of tumors [8, 17]. Recently, interstitial laser heating has been performed in clinically in the brain with stereotactic implantation of micro thermocouples to monitor temperature, in the liver with implanted micro thermocouples, and in head and neck cancer with single implanted micro thermocouples [2].

Beside these areas, thermocouples have been used in surgical laser studies to measure temperatures in normal tissues adjacent to the surgical target. Thermocouples have been applied to the studies of thermal effects of Nd:YAG laser irradiation using animal models [8].

In this study, temperature values were measured at different radial and axial distances during laser irradiation from different types of tissues (lamb brain, heart, kidney). The effect of different power levels on different type of tissues were tested *in vitro* by using 980-nm diode laser and tried to make a relation between power levels, measured temperature and photothermal effect. During laser irradiation, thermocouples were used to measure temperatures.

3. MATERIALS AND METHODS

As stated before, the goal of this project is to measure the temperature values at different radial and axial distances during laser irradiation from different types of tissues. According to obtained results, optimum parameters will be determined to minimize thermal damage to the neighborhood of target tissue.

3.1 Laser System

In this study, 980-nm diode laser (OPC-D010-980-FCPS, Opto Power Corporation, Tuscon, AZ, USA) was the light source under the permission of Prof.Dr. İnci Çilesiz, İstanbul Technical University. A fiber optic probe was used to apply the laser light to the tissue (Figure 3.1).

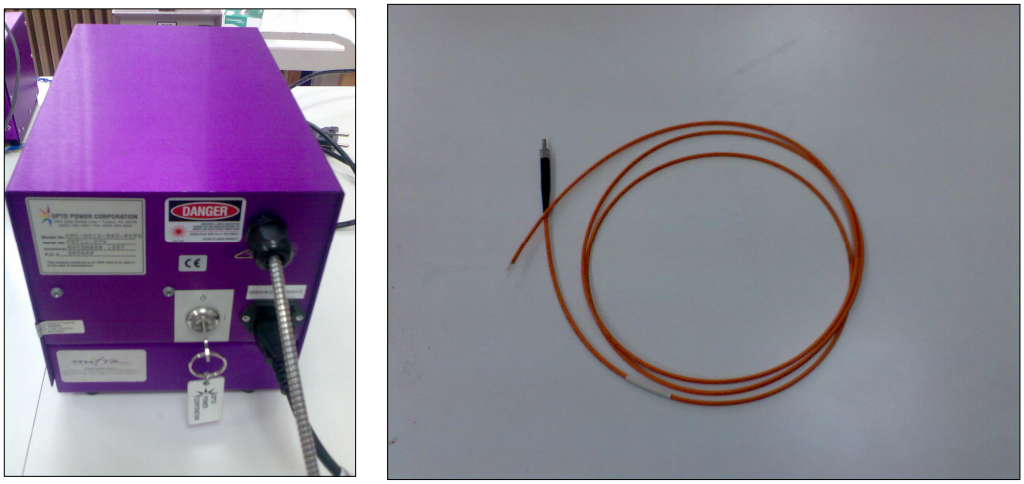

(a) (b)

Figure 3.1 Laser system. (a) 980-nm diode laser, (b) Fiber optic probe

The laser system was connected to the computer by using an RS 232 cable and the laser parameters were adjusted by using the laser interface (Figure 3.2). While the amounts of duty cycle, off cycle and number of cycle were adjusted directly, the output power levels of the laser were determined according to previously defined current values (10A → 2W, 13A → 3W, 16A → 4W).

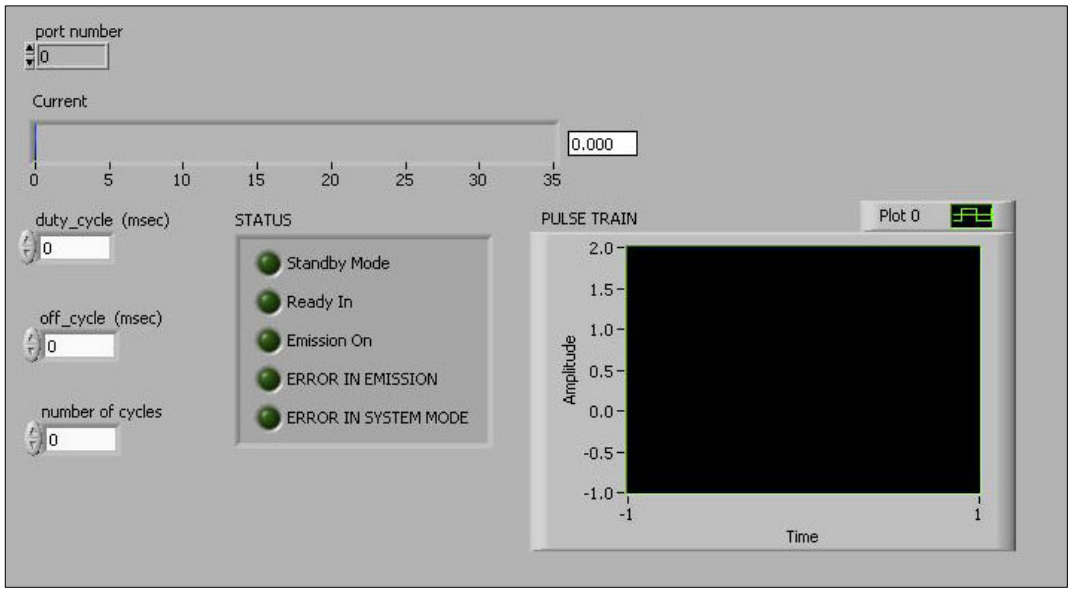

Figure 3.2 Laser interface. Laser parameters (duty cycle, off cycle, number of cycles) were adjusted by using this interface. To determine the power levels, previously defined current values were used.

The laser parameters which were used in this experiment are shown in Table 3.1.

Table 3.1
Laser Parameters

Duty Cycle	500 ms
Off Cycle	500 ms
Number of Cycle	20
Power	2W, 3W,4W

3.2 Tissue Preparation

Fresh lamb kidney, brain and heart were obtained from a local butcher. The fresh lamb kidney was cut into two equal parts and the outer shell cortex was divided into rectangular slabs with a dimension of 1cm x 2cm and thickness of 1-2cm. The cortex was the first part of the slab which interacts with the laser beam. The cortex of fresh lamb brain was divided into rectangular slabs with a dimension of 1cm x 2cm and thickness of 1 -2cm. The endocardium of the heart tissue was prepared like kidney and brain cortex.

For 3-mm and 5-mm deep measurements, thermocouple needles were inserted in the cerebrum, and the laser beam was applied to the cortex.

3.3 Temperature Measurement System

In this study, thermocouple was used as temperature measuring device during laser irradiation. As mentioned before, 980-nm diode laser was the light source. 6 thermocouple probes were connected to 8 channel thermocouple temperature recorder (OM- CP-OCTTEMP, Omega, Man., UK) (Figure 3.3). This temperature recorder was connected to personal computer by using an RS 232 cable and the values were evaluated with Omega Engineering data recording software (Figure 3.4).

The thermocouple temperature recorder are used to measure ambient temperature and 8 different temperature values. For this device, the thermocouple type is K, the tip diameter of thermocouple probe is 1-mm and temperature measurement ranges between -270ºC and 1370ºC. For 1-mm diameter probe tip, response time is 0.25 second. All these equipments are available at Biophotonics Laboratory of Institute of Biomedical Engineering, Bogazici University.

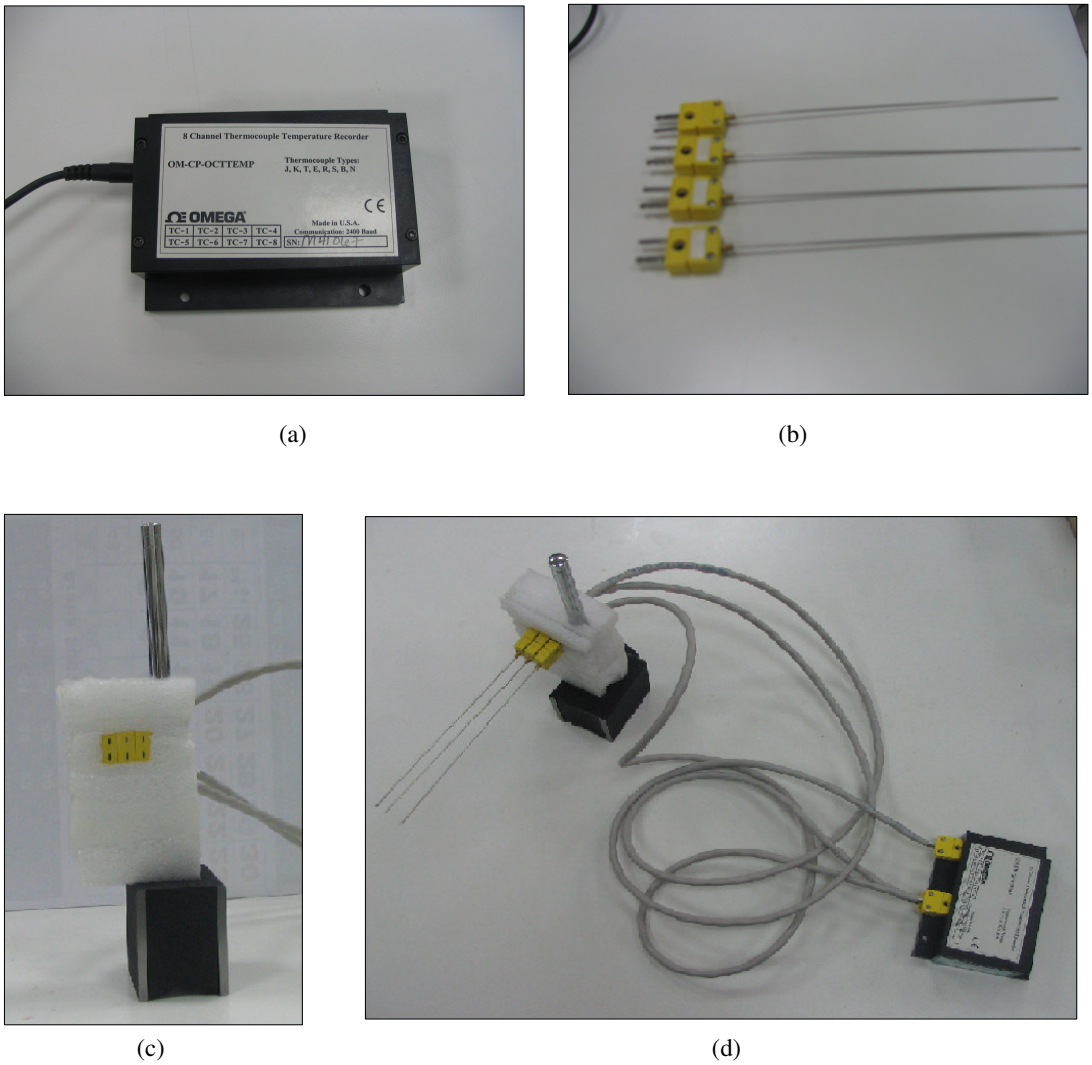

Figure 3.3 Temperature measurement system. (a) 8 channel thermocouple temperature recorder (b) Thermocouple probes, (c) The view of fixed places to hold thermocouple probes, (d) Thermocouple temperature recorder with probes.

Figure 3.4 The interface of Omega Engineering data recording software

3.4 Experimental Setup

For 3-mm and 5-mm deep measurements, 3cm x 3cm x 2cm dimensions and frontal side and upper side opened wooden cube was used (Figure 3.5). Tissue samples were placed inside the cube. To hold thermocouple probes inside tissues regularly, drilled acetate was put on the front side of the cube. Thermocouple needles were inserted to the tissues via regularly drilled acetate as parallel to surface. At the experimental setup, magnetic bases were used to hold optical fiber and thermocouple probes fixed (Figure 3.5c). The laser was applied to the tissue in the direction of the middle probe.

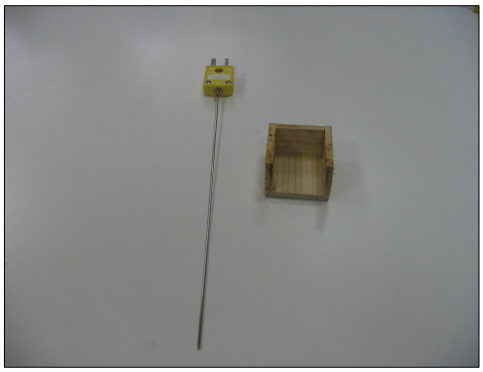

(a)

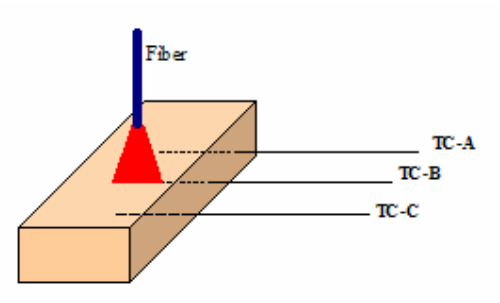

(b)

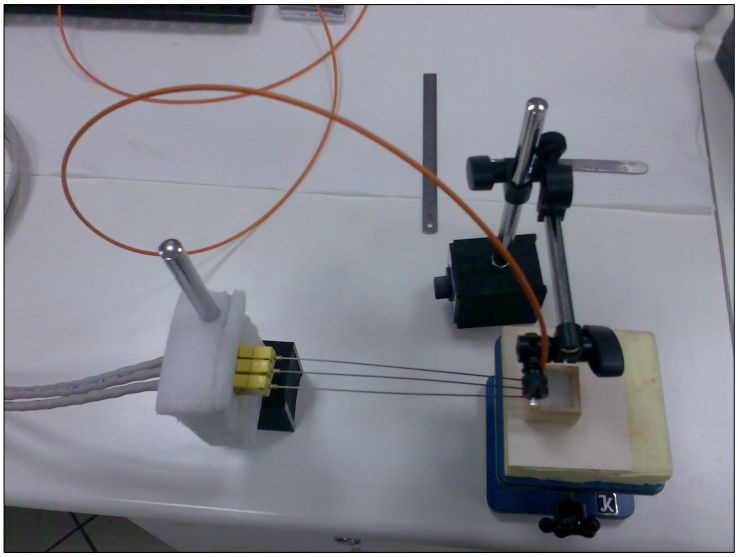

(c)

Figure 3.5 Deep temperature measurement system. (a) Previously prepared wooden cube (b) Putting the probes inside the tissue. (c) The whole view of the deep temperature measurement system.

The deep measurements were realized at two steps. At the first step, 3 thermocouple probes were placed at 3-mm depth from the surface of the tissue. This thermocouple array was parallel to the surface. The distances between thermocouple probes were 3-mm. The laser was applied to the upper part of the tissue with 2-mm spot size. At the second step, the same experimental setup was repeated to measure tissue temperature at the 5-mm depth from the surface of the tissue.

4. RESULTS

4.1 3-mm Deep Measurement

The ability to accurately measure the temperature value of laser-heated biological tissue with thermocouple is affected by direct absorption of laser energy into the sensor itself [8, 10, 17]. To determine the level of direct absorption by thermocouple needles, laser was applied to the system when there were no tissue samples at the experimental setup and temperature measurements were done.

The results of temperature measurement when there were no tissue samples at the experimental setup are shown in Table 4.1.

Table 4.1
The results of temperature measurements without any tissue samples at the experimental setup

2W Laser Irradiation	First Temperature *ºC*	Last Temperature *ºC*	Increase *ºC*
TC-A	25.56	26.61	1.05
TC-B	25.615	27.14	1.525
TC-C	25.525	26.255	0.73
3W Laser Irradiation			
TC-A	25.76	27.11	1.35
TC-B	25.695	27.725	2.03
TC-C	25.665	26.4	0.735
4W Laser Irradiation			
TC-A	25.73	27.395	1.67
TC-B	25.69	28.36	2.67
TC-C	25.605	26.66	1.06

After measuring temperature values when there were no tissue samples at the experimental setup, the measurement process was repeated with tissues. For this purpose lamb brain, heart and kidney were used as the tissue samples. 980-nm diode laser was used as the light source at different power levels (2W, 3W, 4W).

As stated before, for 3-mm deep measurement, frontal side and upper side opened wooden cube at 3cm x 3cm x 2cm dimensions was used. Temperature measurements were done by inserting the thermocouple probes inside tissues at 3-mm depth from the surface, (here, the distance between thermocouple probes are 3-mm and the laser was applied from the upper part of the tissue with 2-mm spot size).

By using these parameters, 8 different experiments were done for each situation. The results are shown in Table 4.2. The values in the table are the average of the 8 different experimental results.

Table 4.2
Temperature measurements at 3-mm depth from the surface. (a) Lamb brain, (b) Lamb kidney, (c) Lamb heart

Lamb Brain

2W Laser Irradiation	First Temperature *ºC*	Last Temperature *ºC*	Increase *ºC*
TC-A	20.97	22.54	1.57
TC-B	20.90	28.91	8.01
TC-C	20.93	22.65	1.72
3W Laser Irradiation			
TC-A	21.26	23.87	2.61
TC-B	21.22	34.16	12.94
TC-C	21.22	23.44	2.22
4W Laser Irradiation			
TC-A	21.17	24.37	3.2
TC-B	21.11	37.48	16.37
TC-C	21.17	23.92	2.75

(a)

Lamb Kidney

2W Laser Irradiation	First Temperature *ºC*	Last Temperature *ºC*	Increase *ºC*
TC-A	18.7	20.8	2.1
TC-B	18.65	26.63	7.98
TC-C	18.6	20.43	1.83
3W Laser Irradiation			
TC-A	19.03	21.58	2.55
TC-B	18.96	29.36	10.4
TC-C	19.01	21.78	2.77
4W Laser Irradiation			
TC-A	18.86	22.58	3.72
TC-B	18.9	33.57	14.67
TC-C	18.88	22.59	3.71

(b)

Lamb Heart

2W Laser Irradiation	First Temperature *ºC*	Last Temperature *ºC*	Increase *ºC*
TC-A	21.17	22.42	1.25
TC-B	21.12	27.45	6.33
TC-C	21.21	22.63	1.42
3W Laser Irradiation			
TC-A	21.59	23.60	2.01
TC-B	21.51	30.96	9.45
TC-C	21.64	23.63	1.99
4W Laser Irradiation			
TC-A	21.8	24.53	2.73
TC-B	21.76	34.65	12.89
TC-C	21.77	24.61	2.84

(c)

By using the data in the above tables, the temperature increments of the tissue samples at 3-mm depth from the surface are shown in Figure 4.1.

In these figures, the temperature increments, laser powers and the distances to the laser target were compared.

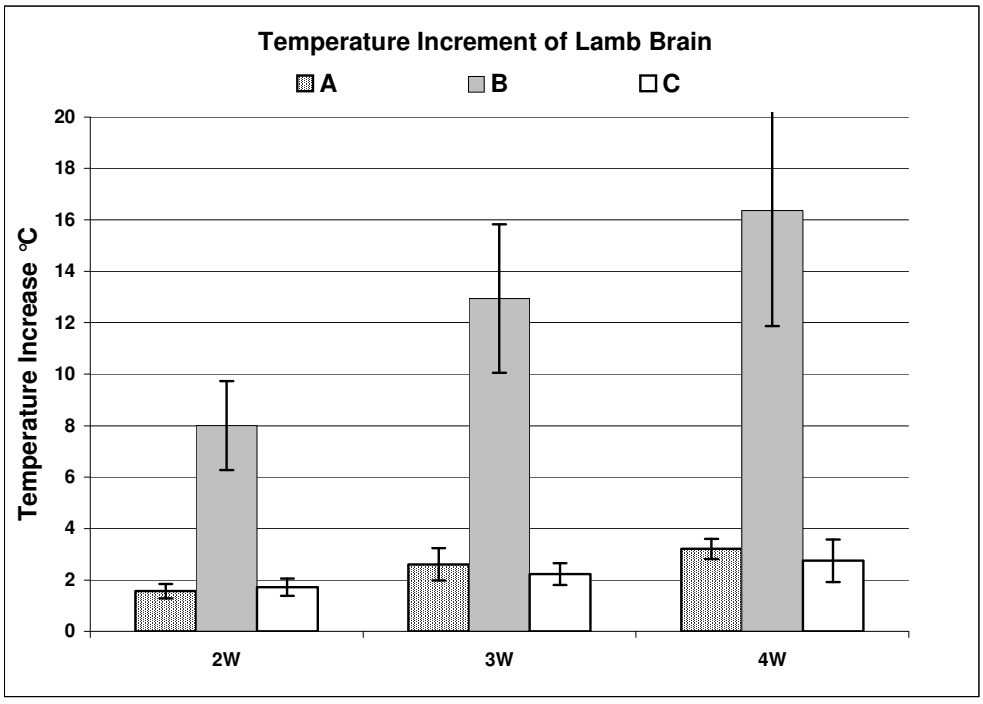

(a)

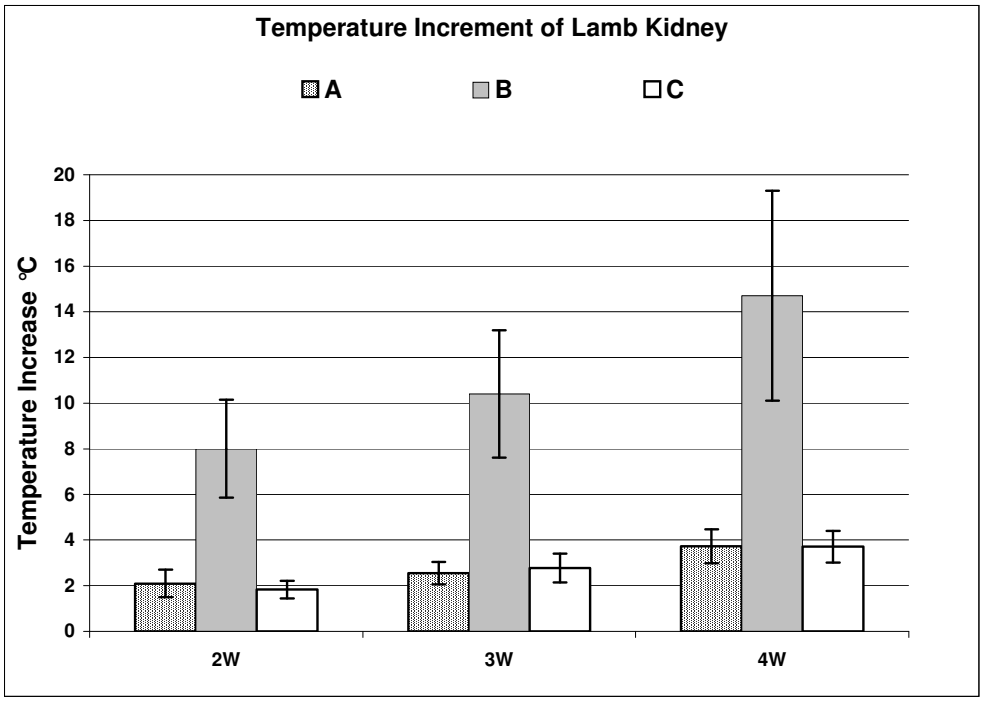

(b)

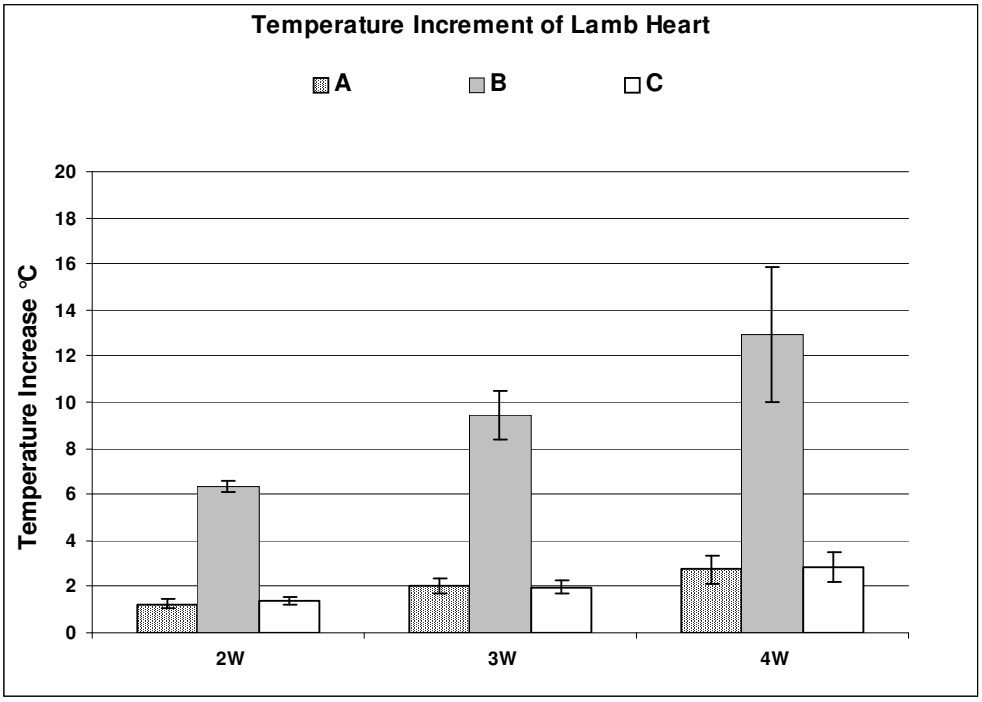

(c)

Figure 4.1 3-mm deep point temperature measurements. B(TC-B) is the middle thermocouple probe and A(TC-A) and C(TC-C) are the side thermocouple probes. The distances between thermocouple probes were 3-mm. The laser was applied to the direction of the middle probe (TC-B) and the spot size was 2-mm. (a) Lamb brain, (b) Lamb kidney, (c) Lamb heart.

When the above figures were taken into account, as a result of the t-test, the probability values between TC-A – TC-B and TC-B – TC-C are lower than 0.05 ($p<0.05$) and the probability value for TC-A – TC-C is higher than 0.05 ($p>0.05$). This is applicable for 3 types of tissue (lamb brain, heart and kidney). Therefore, while there is a statistical difference between measured temperatures of middle thermocouple (TC-B) and side thermocouples (TC-A, TC-C), there is no statistical difference between the measured temperatures of the side thermocouples. Second, when the statistical test was applied to the measured temperature values at different power levels, it was observed that the probability values between different power levels (2W-3W, 3W-4W, 2W-4W) are lower than 0.05 ($p<0.05$). It means that, the measured temperature values for different laser output power levels are statistically different from each other. This is valid for 3 types of tissues.

Laser energy at different power levels has different effects on the tissue samples. A comparison of temperature increments on lamb brain, kidney and heart at 3-mm depth from the surface during laser irradiation are given in Figure 4.2.

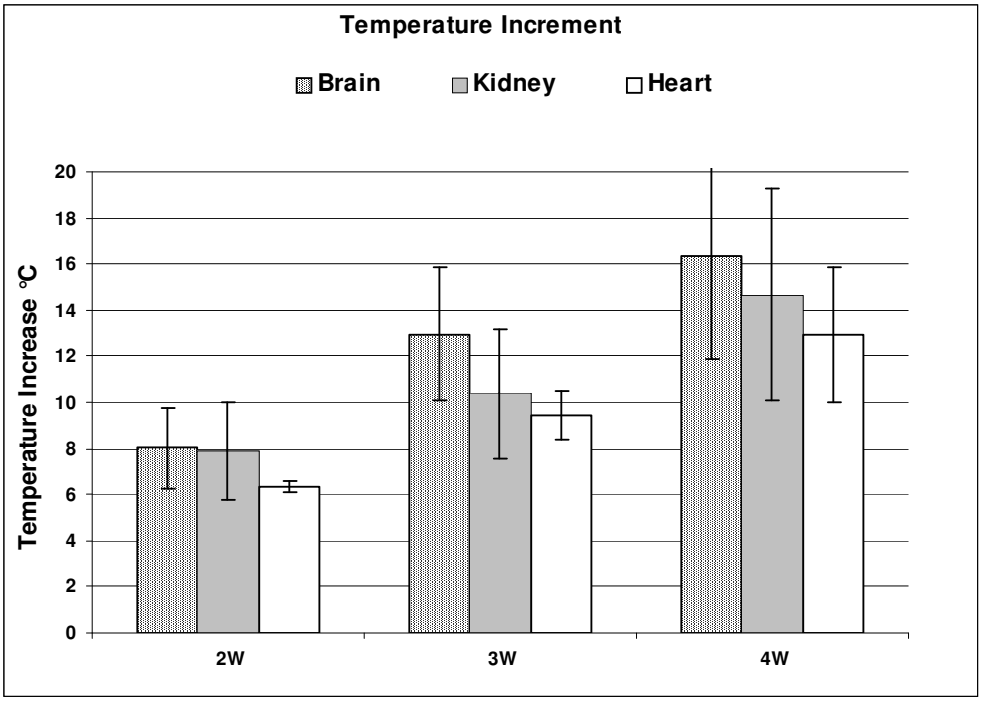

Figure 4.2 During the laser irradiation at different power levels, the temperature increment of the certain tissues at 3-mm deep point. These are the measured values which obtained from the middle thermocouple probe (TC-B).

To determine whether there is a statistical difference between temperature increments of different types of tissues, t-test was applied. As a result of this test, it was observed that the probability value between the measured temperature of brain and heart tissue at 2W and 3W laser output power levels is lower than 0.05 ($p<0.05$), but it is higher than 0.05 ($p>0.05$) at 4W laser output power level. The probability value between brain and kidney tissues is higher than 0.05 ($p>0.05$) at all laser output power levels. Also the probability value between the measured temperatures of kidney and heart tissues is higher than 0.05 ($p>0.05$) at all laser output power levels. Therefore, while there is a statistical difference between the temperature increment of brain and heart tissue at 2W and 3W laser output power levels, there is no statistical difference between the temperature increments of brain and kidney tissue, and kidney and heart tissue at different power levels.

4.2 5-mm Deep Measurement

Temperatures at 5-mm dept from the surface of the tissues were measured by using the same experimental setup (3-mm deep measurement). For these purpose, frontal side and upper side opened wooden cube at 3cm x 3cm x 2cm dimensions was used. The frontal side of the wooden cube was closed with the drilled acetate to hold the thermocouple probes regularly at 5-mm dept from the surface.

The distances between thermocouple probes were 3-mm and the laser was applied to the upper part of the tissue with 2-mm spot size.

By using these parameters, 8 different experiments were done for each situation (for different tissue samples and for different power values). The results are shown in Table 4.3. The values in the table are the average of the 8 different experimental results.

Table 4.3
Temperature measurements at 5-mm depth from the surface. (a) Lamb brain, (b) Lamb kidney, (c) Lamb heart

Lamb Brain

2W Laser Irradiation	First Temperature *ºC*	Last Temperature *ºC*	Increase *ºC*
TC-A	17.08	17.97	0.89
TC-B	17	19.15	2.15
TC-C	17.03	18.02	0.99
3W Laser Irradiation			
TC-A	17.12	18.42	1.3
TC-B	17.04	20.06	3.02
TC-C	17.12	18.24	1.12
4W Laser Irradiation			
TC-A	17.22	19.46	2.24
TC-B	17.08	22.62	5.54
TC-C	17.36	19.24	1.88

(a)

Lamb Kidney

2W Laser Irradiation	First temperature *ºC*	Last Temperature *ºC*	Increase *ºC*
TC-A	21.09	22.17	1.08
TC-B	21.14	23.54	2.4
TC-C	21.18	22.29	1.11
3W Laser Irradiation			
TC-A	21.07	22.7	1.63
TC-B	21.09	24.54	3.45
TC-C	21.21	22.76	1.55
4W Laser Irradiation			
TC-A	21.49	23.74	2.25
TC-B	21.6	26.26	4.66
TC-C	21.65	23.96	2.31

(b)

Lamb Heart

2W Laser Irradiation	First Temperature *ºC*	Last Temperature *ºC*	Increase *ºC*
TC-A	15.62	16.41	0.79
TC-B	15.49	17.19	1.7
TC-C	15.45	16.25	0.8
3W Laser Irradiation			
TC-A	15.76	17.09	1.33
TC-B	15.78	18.6	2.82
TC-C	15.81	17.07	1.26
4W Laser Irradiation			
TC-A	15.65	17.26	1.61
TC-B	15.57	18.95	3.38
TC-C	15.58	17.24	1.66

(c)

By using the data in Table 4.3, the temperature increments of tissue samples at 5-mm depth from the surface are shown in Figure 4.3.

In these figures, the temperature increments, laser powers and the distances to the laser target were compared.

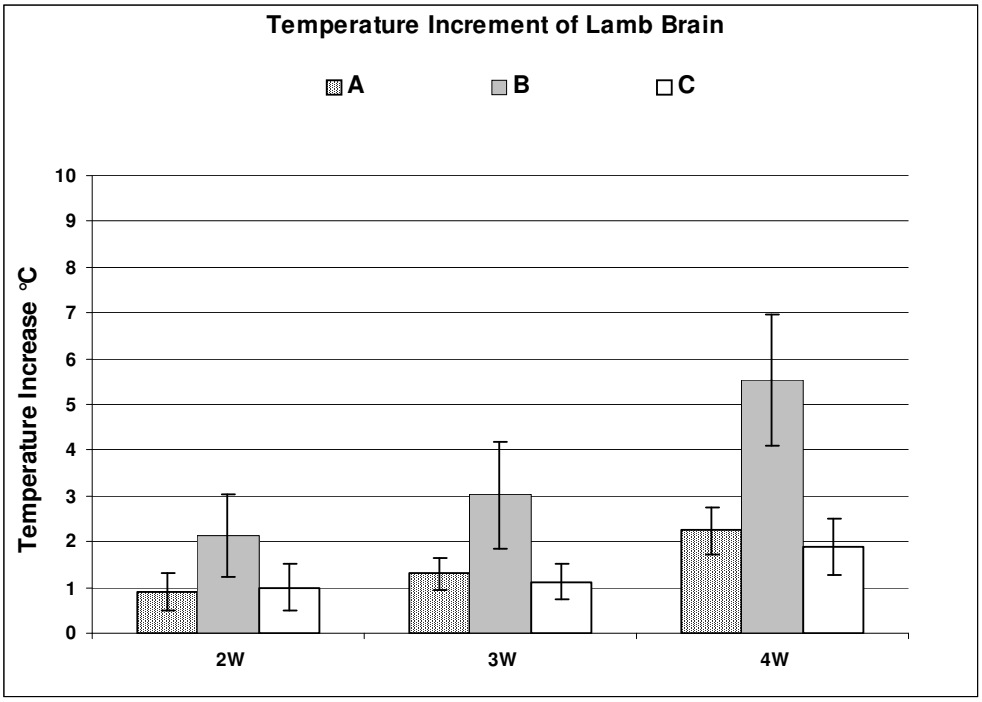

(a)

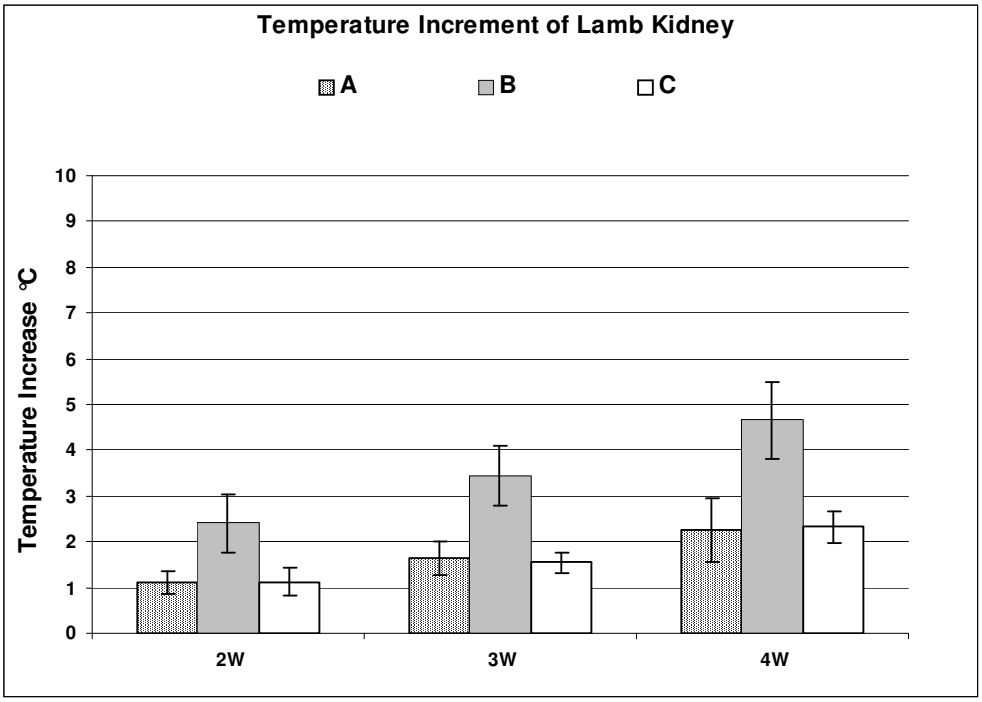

(b)

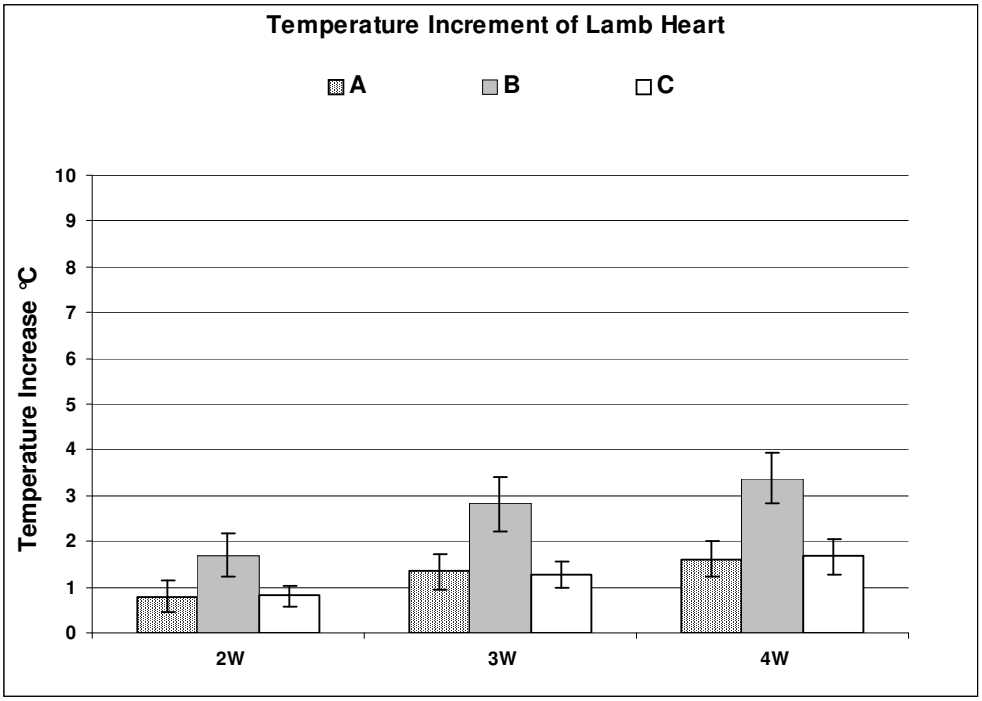

(c)

Figure 4.3 5-mm deep point temperature measurements. B(TC-B) is the middle thermocouple probe and A(TC-A) and C(TC-C) are the side thermocouple probes. The distances between thermocouple probes were 3-mm. The laser was applied to the direction of the middle probe (TC-B) and the spot size was 2-mm. (a) Lamb brain, (b) Lamb kidney, (c) Lamb heart.

When the above figures were taken into account, as a result of the t-test, the probability values between TC-A – TC-B and TC-B – TC-C are lower than 0.05 ($p<0.05$) and the probability value for TC-A – TC-C is higher than 0.05 ($p>0.05$). This is applicable for 3 types of tissues (lamb brain, heart and kidney). Therefore, while there is a statistical difference between measured temperatures of middle thermocouple (TC-B) and side thermocouples (TC-A, TC-C), there is no statistical difference between the measured temperatures of the side thermocouples. Second, when the statistical test was applied to the measured temperature values at different power levels, it was observed that the probability value between different power levels (2W-3W, 3W-4W, 2W-4W) is lower than 0.05 ($p<0.05$). It means that, the measured temperature values at different laser output power levels are statistically different from each other. This is valid for 3 types of tissues.

During laser tissue interaction, laser energy at different power levels has different effects on the tissue samples. A comparison of temperature increment on lamb brain, kidney and heart at 5-mm depth from the surface during laser irradiation are given in Figure 4.4.

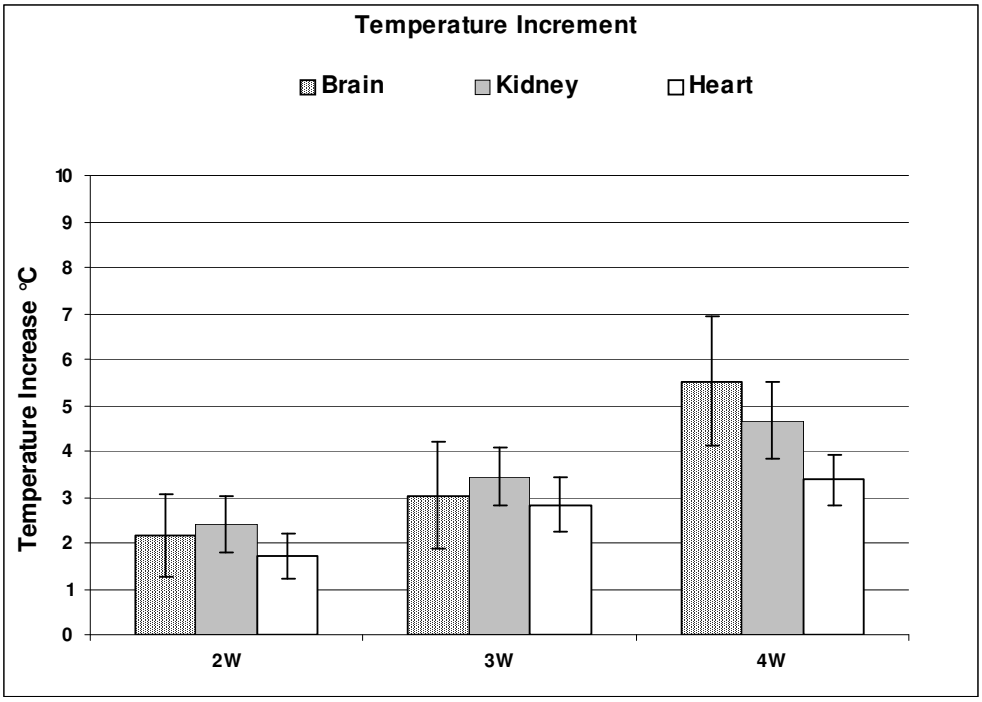

Figure 4.4 During the laser irradiation at different power levels, the temperature increment of the certain tissues at 5-mm deep point. These are the measured values which obtained from the middle thermocouple probe (TC-B).

To determine whether there is a statistical difference between temperature increments of different types of tissues, t-test was applied. As a result of the test, it was observed that the probability value between the measured temperature of brain and heart tissues at 4W laser output power level is lower than 0.05 ($p<0.05$) but this value is higher than 0.05 at 2W and 3W power levels. The probability value between the measured temperature of brain and kidney tissues is higher than 0.05 ($p>0.05$) at all laser output power levels. Therefore, while there is a statistical difference between the temperature increment of brain and heart tissue and kidney and heart tissue at 4W laser output power levels, no statistical difference exists at 2W and 3W laser output power levels. Also, there

is no statistical difference between the temperature increments of brain and kidney tissue at all power levels (2W, 3W, 4W).

In the above figures, temperature increases are shown depending on the laser output power levels and the distance from the target point of laser light. By using *MATLAB* and *surf* command, temperature increments depending on the time and distances are shown in the below figures as three dimensional plotting.

3-mm deep measurement

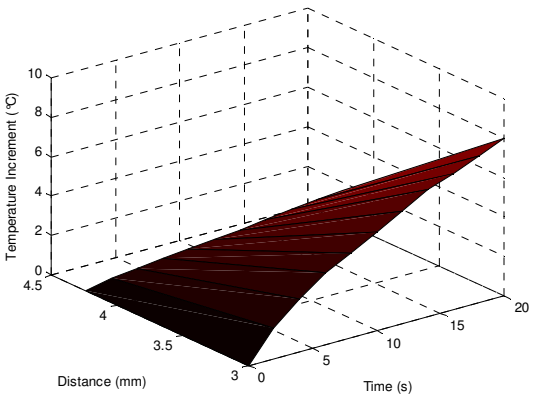

(a)

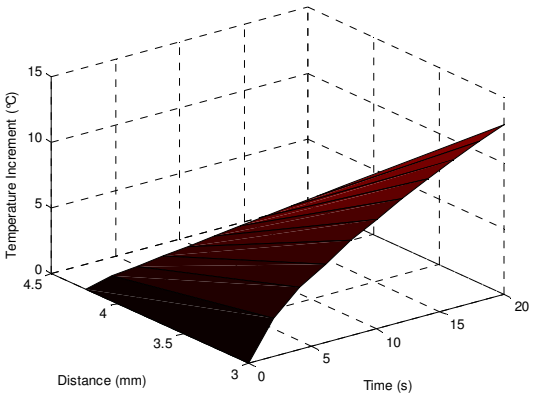

(b)

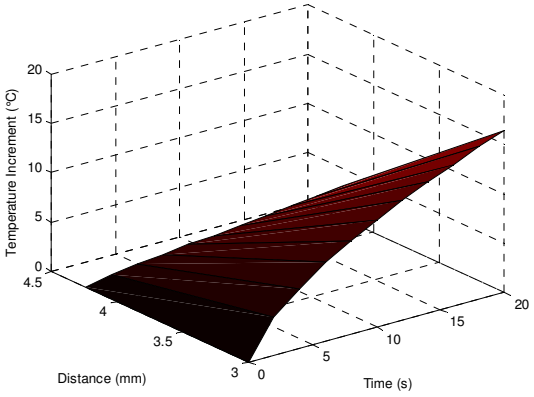

(c)

Figure 4.5 For 3-mm deep measurement of brain tissue, three dimensional plotting of the temperature increment depending on time and distances. The time changes from 0 to 20s with 2 seconds steps; the distance is 3-mm from the surface in the direction of the laser target point for the middle thermocouple, and 4.24-mm (not in the direction of laser target point) for the side thermocouples. (a) 2W, (b) 3W, (c) 4W

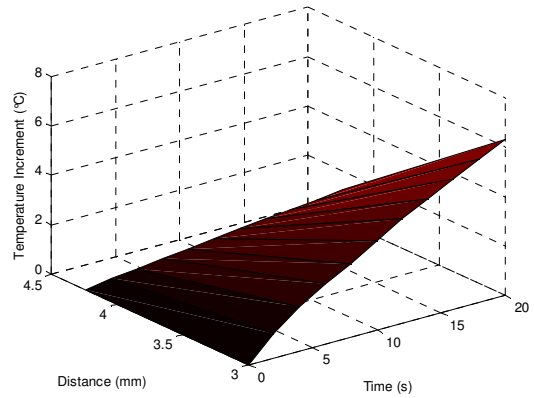

(a)

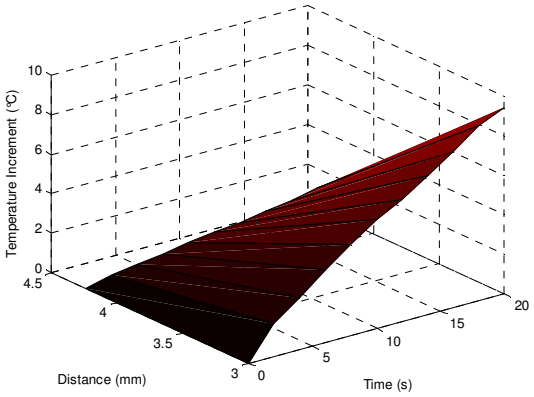

(b)

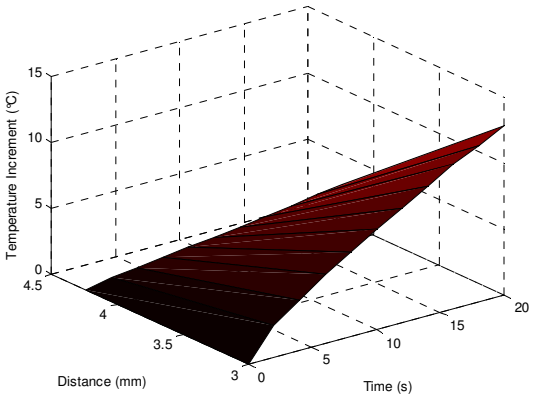

(c)

Figure 4.6 For 3-mm deep measurement of heart tissue, three dimensional plotting of the temperature increment depending on time and distances. The time changes from 0 to 20s with 2 seconds steps; the distance is 3-mm from the surface in the direction of the laser target point for the middle thermocouple, and 4.24-mm (not in the direction of laser target point) for the side thermocouples. (a) 2W, (b) 3W, (c) 4W

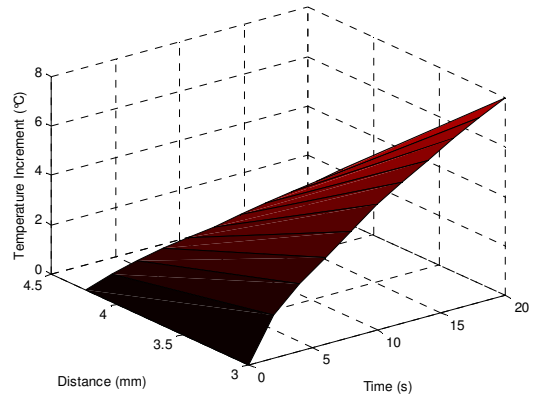

(a)

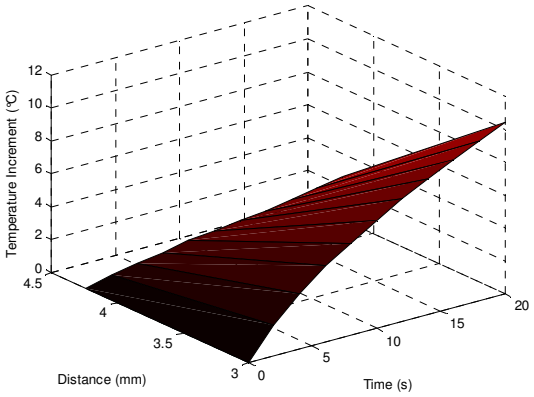

(b)

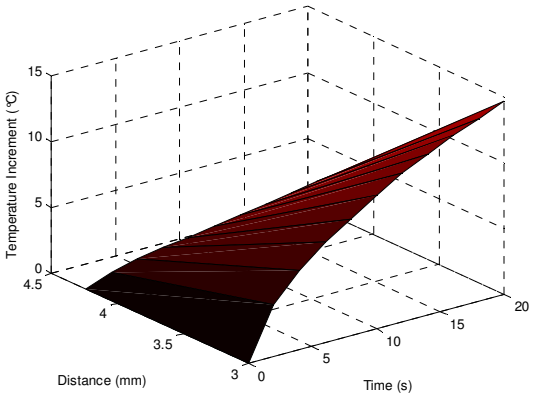

(c)

Figure 4.7 For 3-mm deep measurement of kidney tissue, three dimensional plotting of the temperature increment depending on time and distances. The time changes from 0 to 20s with 2 seconds steps; the distance is 3-mm from the surface in the direction of the laser target point for the middle thermocouple, and 4.24-mm (not in the direction of laser target point) for the side thermocouples. (a) 2W, (b) 3W, (c) 4W

5-mm deep measurement

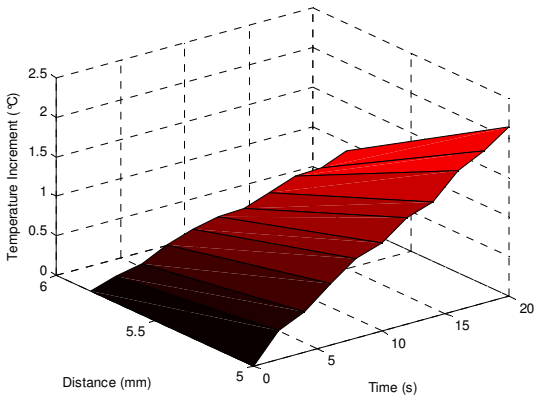

(a)

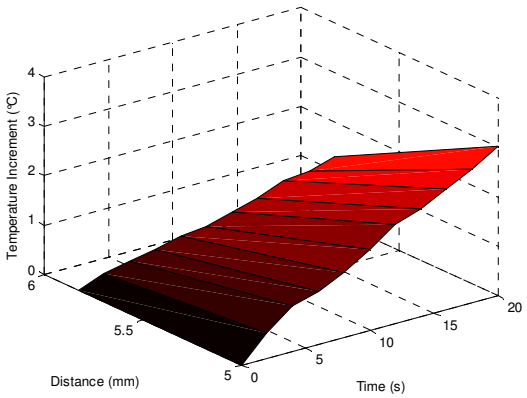

(b)

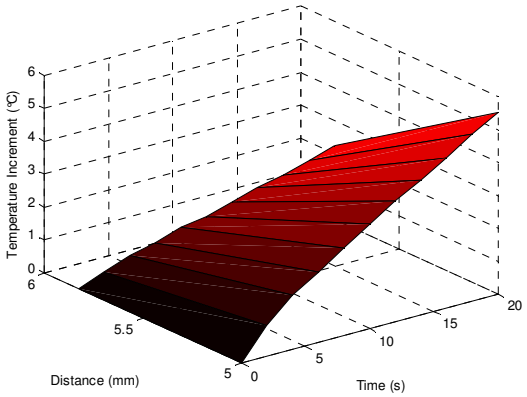

(c)

Figure 4.8 For 5-mm deep measurement of brain tissue, three dimensional plotting of the temperature increment depending on time and distances. The time changes from 0 to 20s with 2 seconds steps; the distance is 5-mm from the surface in the direction of the laser target point for the middle thermocouple, and 5.83-mm (not at the direction of laser target point) for the side thermocouples. (a) 2W, (b) 3W, (c) 4W

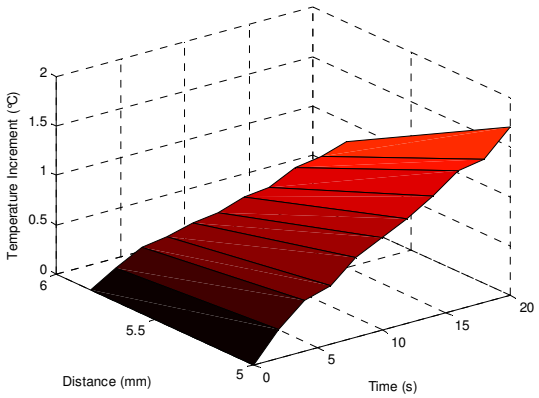

(a)

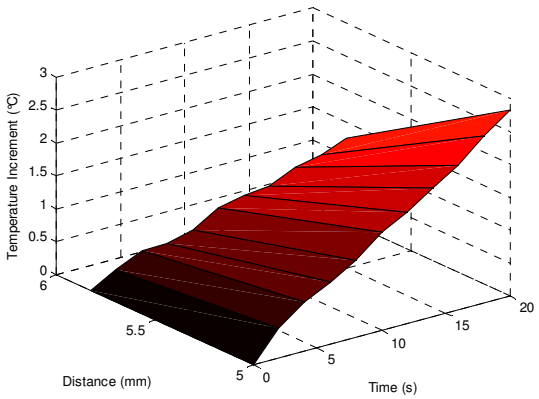

(b)

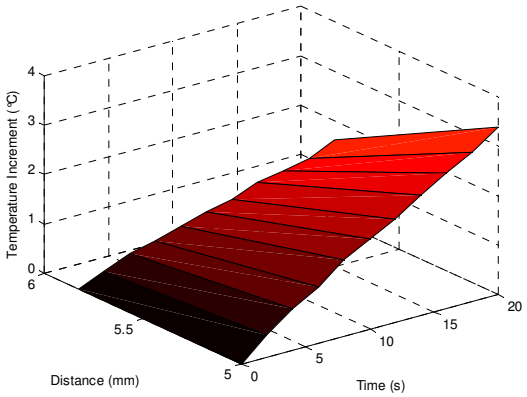

(c)

Figure 4.9 For 5-mm deep measurement of heart tissue, three dimensional plotting of the temperature increment depending on time and distances. The time changes from 0 to 20s with 2 seconds steps; the distance is 5-mm from the surface in the direction of the laser target point for the middle thermocouple, and 5.83-mm (not in the direction of laser target point) for the side thermocouples. (a) 2W, (b) 3W, (c) 4W

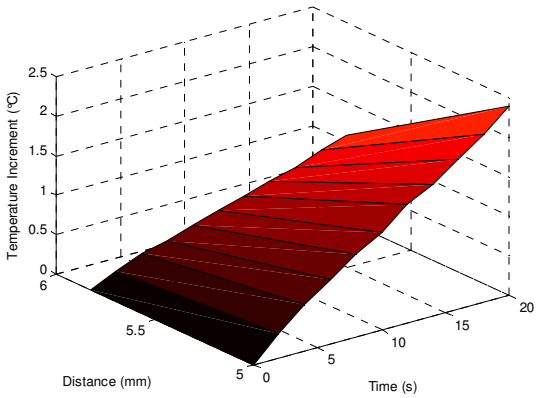

(a)

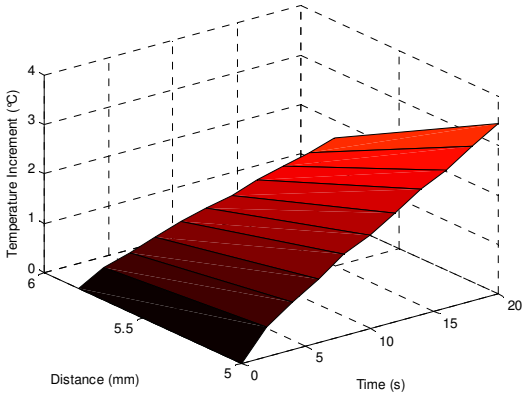

(b)

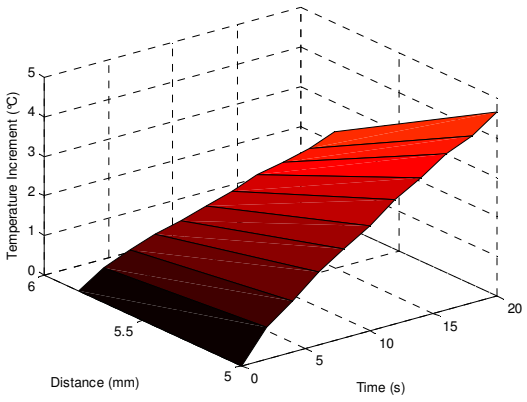

(c)

Figure 4.10 For 5-mm deep measurement of kidney tissue, three dimensional plotting of temperature increment depending on time and distances. The time changes from 0 to 20s with 2 seconds steps; the distance is 5-mm from the surface in the direction of the laser target point for the middle thermocouple, and 5.83-mm (not in the direction of laser target point) for the side thermocouples. (a) 2W, (b) 3W, (c) 4W

After showing the temperature increments at 3-mm and 5-mm deep measurements separately, showing a figure which has the correlation of the temperature increments at 3-mm and 5-mm deep measurements will be beneficial to determine the temperature distribution towards the deeper regions of tissues. For this reason, the measured values of the middle thermocouple (TC-B) at 3-mm and 5-mm deep measurements were taken into account to plot the three dimensional graph. In the below figures, three dimensional plotting of temperature increments at 3-mm and 5-mm deep measurements are given and the correlation between these two values are shown.

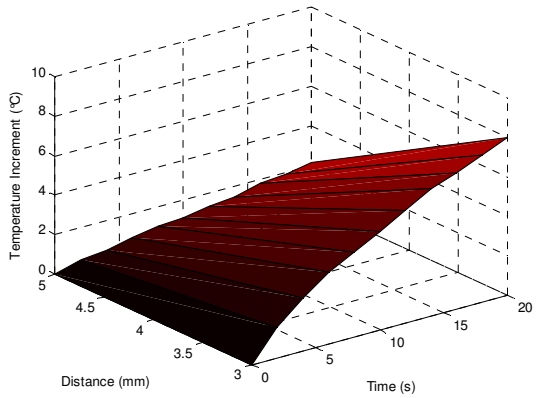

(a)

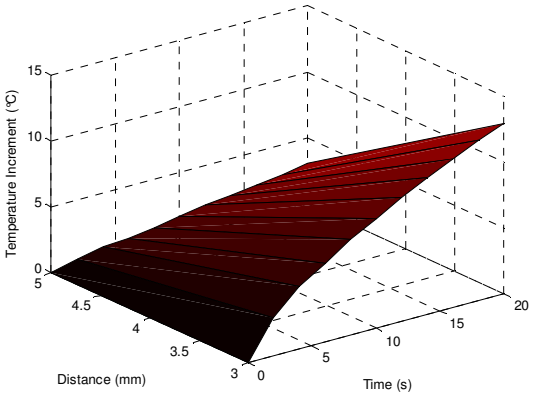

(b)

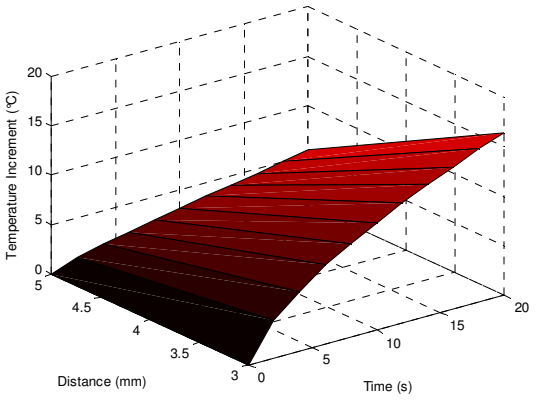

(c)

Figure 4.11 The correlation between 3-mm and 5-mm deep measurements of brain tissue (by using the measured temperature values of middle thermocouple probe – TC-B), three dimensional plotting of temperature increment depending on time and distances. The time changes from 0 to 20s with 2 seconds steps; the distance changes from 3-mm to 5-mm depth from the surface in the direction of the laser target point. (a) 2W, (b) 3W, (c) 4W.

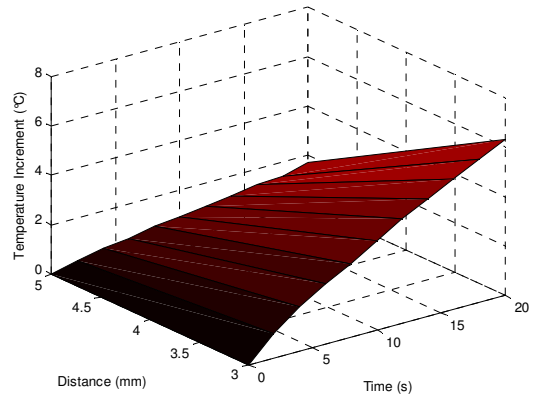

(a)

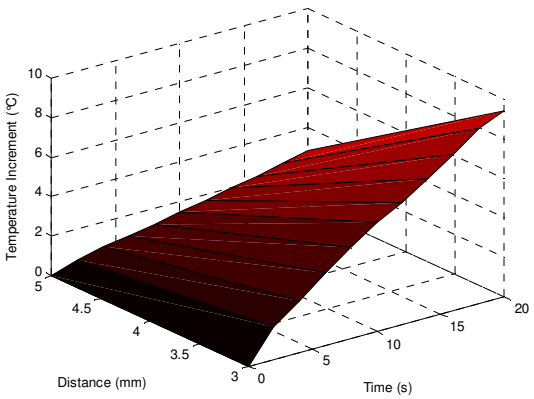

(b)

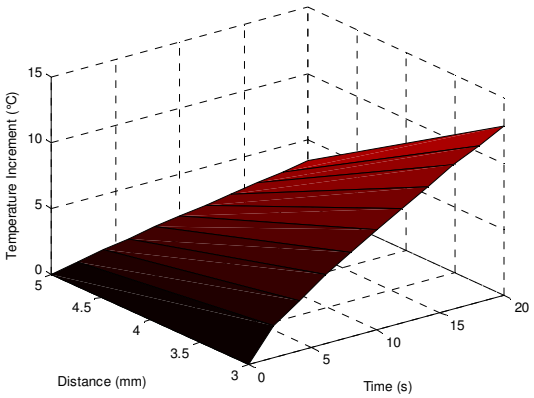

(c)

Figure 4.12 The correlation between 3-mm and 5-mm deep measurements of heart tissue (by using the measured temperature values of middle thermocouple probe – TC-B), three dimensional plotting of temperature increment depending on time and distances. The time changes from 0 to 20s with 2 seconds steps; the distance changes from 3-mm to 5-mm depth from the surface in the direction of the laser target point. (a) 2W, (b) 3W, (c) 4W.

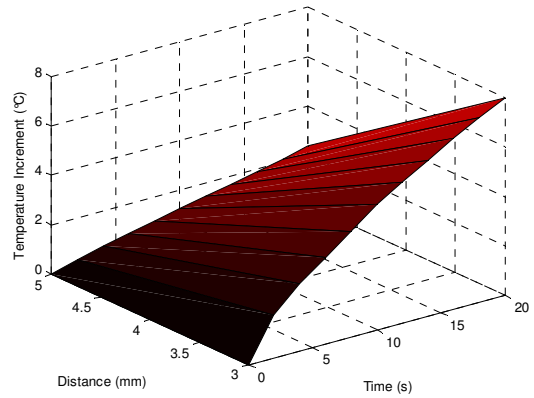

(a)

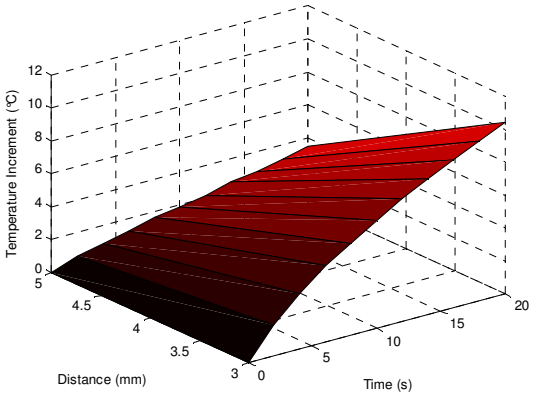

(b)

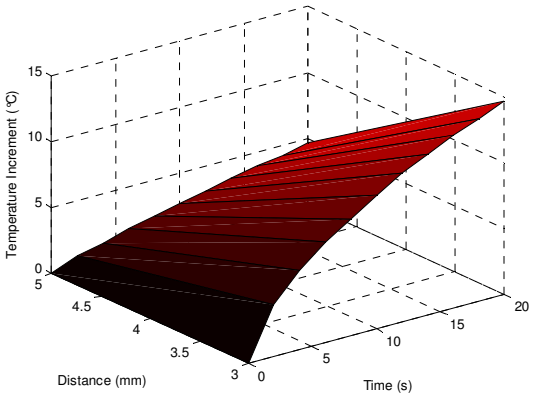

(c)

Figure 4.13 The correlation between 3-mm and 5-mm deep measurements of kidney tissue (by using the measured temperature values of middle thermocouple probe – TC-B), three dimensional plotting of temperature increment depending on time and distances. The time changes from 0 to 20s with 2 seconds steps; the distance changes from 3-mm to 5-mm depth from the surface in the direction of the laser target point. (a) 2W, (b) 3W, (c) 4W.

In the above figures, temperature distributions on tissues during laser irradiation are shown separately at 3-mm and 5-mm deep measurements and then the correlation between 3-mm and 5-mm deep measurements are shown. To get an idea about how temperature disperses on tissue towards the deeper region, showing a figure which contains the measured temperature values at 3-mm and 5-mm deep parts of tissues will be useful. For this purposes, temperature distributions on tissues during laser irradiation for different laser output power levels (2W, 3W, 4W) are shown in the below figures.

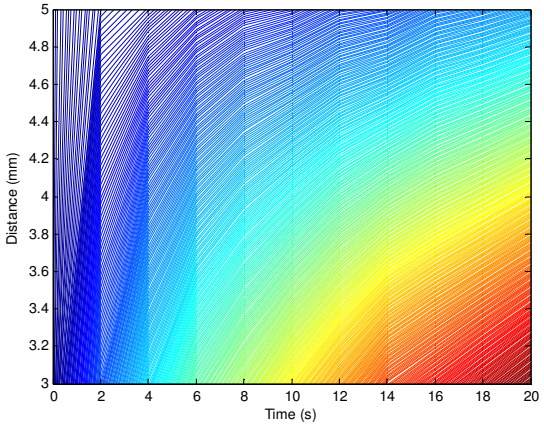

(a)

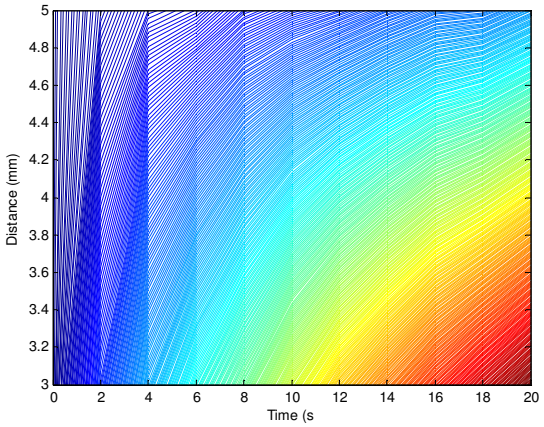

(b)

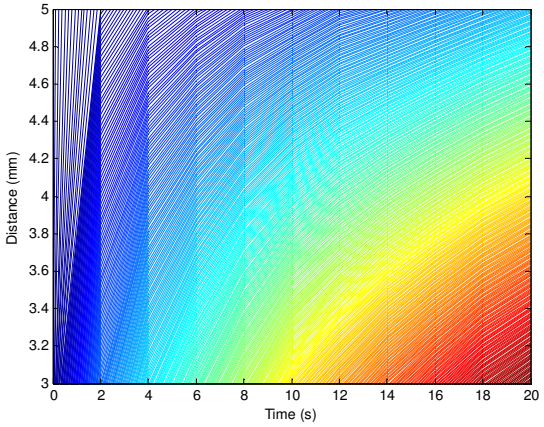

(c)

Figure 4.14 Temperature distributions on tissues at 2W laser output power level. Two thermocouples were used as temperature sensing devices. One of them was placed at 3-mm depth and the other was placed at 5-mm depth from the surface. Both of these thermocouple probes were placed in the direction of the target point of laser irradiation. The time changes from 0 to 20s with 2 seconds steps (a) Brain, (b) Heart,(c) Kidney

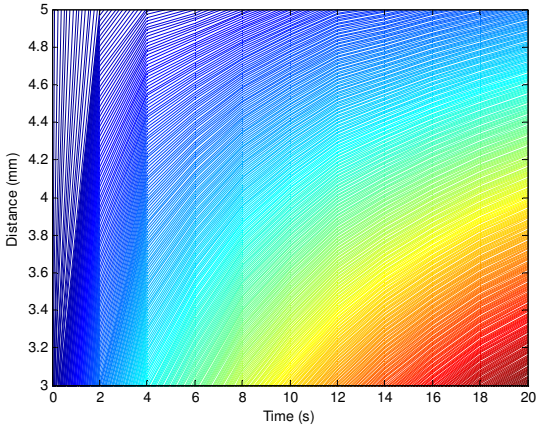

(a)

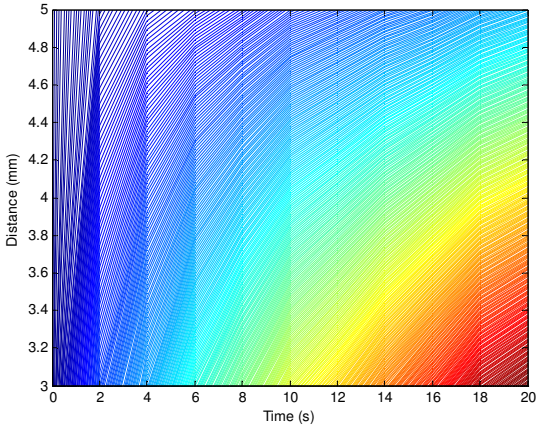

(b)

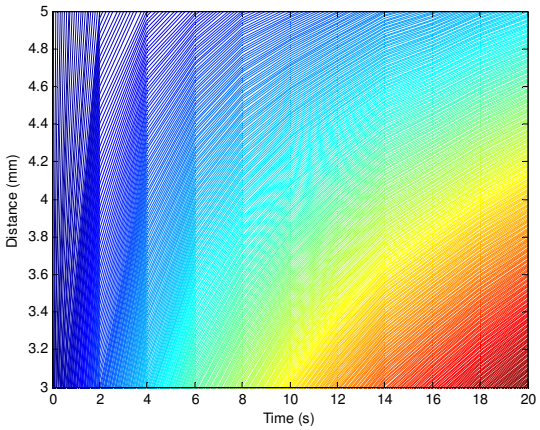

(c)

Figure 4.15 Temperature distributions on tissues at 3W laser output power level. Two thermocouples were used as temperature sensing devices. One of them was placed at 3-mm depth and the other was placed at 5-mm depth from the surface. Both of these thermocouple probes were placed in the direction of the target point of laser irradiation. The time changes from 0 to 20s with 2 seconds steps (a) Brain, (b) Heart,(c) Kidney

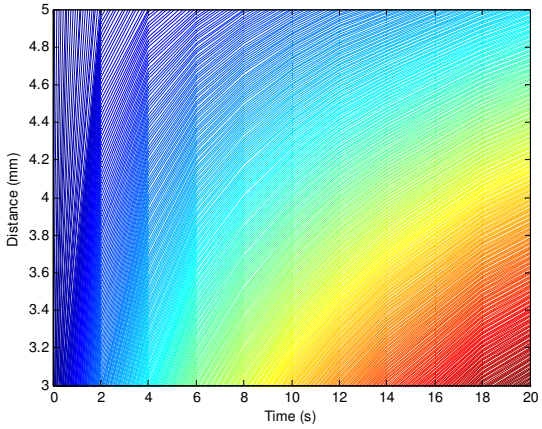

(a)

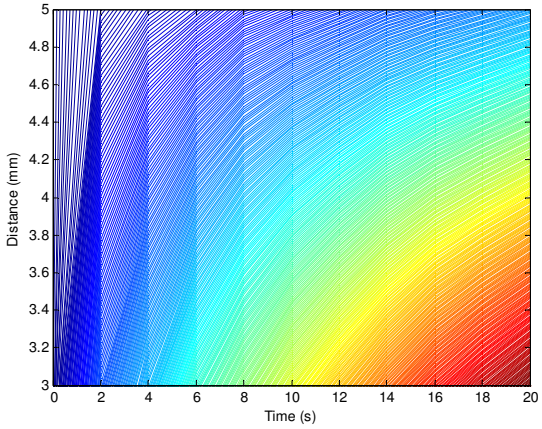

(b)

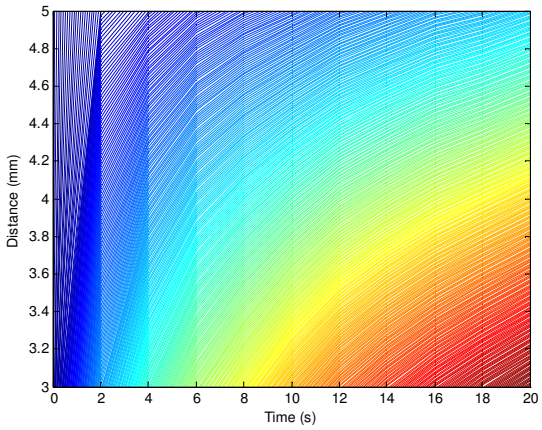

(c)

Figure 4.16 Temperature distributions on tissues at 4W laser output power level. Two thermocouples were used as temperature sensing devices. One of them was placed at 3-mm depth and the other was placed at 5-mm depth from the surface. Both of these thermocouple probes were placed in the direction of the target point of laser irradiation. The time changes from 0 to 20s with 2 seconds steps (a) Brain, (b) Heart,(c) Kidney

5. DISCUSSION AND CONCLUSION

Thermal effect of laser tissue interaction is used at a large part of surgical and clinical applications, which is based on the conversion of optical radiation into thermal energy [8, 10, 13, 17]. The crucial point at these applications is to know the temperature values at different radial and axial distances from the target point of laser irradiation.

The thermal response of tissue to laser irradiation depends on the laser output power level, spot size, the wavelength of the incident light and, optical and thermal properties of the tissue [28].

In this study, with constant spot size (2-mm), the effects of different power levels on certain types of tissues (lamb liver, brain, and kidney) were tested in vitro by using 980-nm diode laser and, a relation between power levels, measured temperature and photothermal effect was shown. As the second duty of the study, the effects of different distances from the target point of laser irradiation on temperature increments were shown. Comparison of the temperature increments of different tissues during laser irradiation was the last focus of the study.

As observed from the figures (in the result section of the study), which display the relation between temperature increments and power levels, temperature increases are linearly positively correlated with the laser output power levels for both 3-mm and 5-mm deep measurements. To determine whether the differences exist as statistically, t-test was applied to the measured temperature values. The probability value between different power levels (2W-3W, 3W-4W, 2W-4W) is less than 0.05 ($p<0.05$). It means that the measured temperatures for different laser output power levels are statistically different from each other. This is valid for 3 types of tissues. For instance, for 3-mm deep measurement of heart tissue, measured temperature increases are 6.33 °C, 9.44 °C, 12.9 °C for 2W, 3W and 4W respectively, for 5-mm deep measurement of heart tissue, measured temperature increases are 1.7 °C, 2.82 °C, 3.37 °C for 2W, 3W and 4W, respectively. Here, temperature increment rate is approximately same for sides and central thermocouples. It means that as the laser output power levels increase, the measured temperatures of parts of the tissue at

different distances from the target point of the laser irradiation increase by the same proportion.

Theoretically, the rate of heat generation S(r) at a position r(r=x,y,z) depends on the values of the local fluence rate and the local absorption coefficient [2]. That is, S(r) is equal to:

$$S(r) = \mu_a(r) * \Phi(r) \quad (5.1)$$

Here,

$\Phi(r)$: the local fluence rate [W/m^2],
μ_a: the local absorption coefficient [1/m] or [m^{-1}]

The total fluence rate includes both the fluence rate of scattered light and the fluence rate of the attenuated collimated laser beam at r.

As observed from the above equation, by increasing the power level on the target point of the tissue, a linear temperature increment occurs at this point. This is true for different distances on the tissue. This situation was observed at both 3-mm and 5-mm deep measurements of tissue during laser tissue interaction.

By taking into account the figures which were shown in the result section of the study, it can be observed that the distances from the target point of laser light has a negative exponential effect on the temperature increases. To control whether a statistical difference exists, t-test was applied to the measured temperature values. As a result of the test, it was seen that the probability values between TC-A – TC-B and TC-B – TC-C are less than 0.05 ($p<0.05$) and the probability value for TC-A – TC-C is higher than 0.05 ($p>0.05$). These situations are valid for 3 types of tissues (lamb brain, heart and kidney). Therefore, while there is a statistical difference between measured temperatures of middle thermocouple (TC-B) and side thermocouples (TC-A, TC-C), there is no statistical difference between the measured temperatures of the side thermocouples. For example, during 4W laser irradiation to the heart tissue, measured temperature increments at 3-mm

deep from the surface are 2.73 °C, 2.83 °C, 12.90 °C for side thermocouples (TC-A, TC-C – 3-mm deep from the surface and 4.24 mm far from the target point of laser irradiation) and central thermocouple (TC-B – 3 mm deep from the surface and on the direction of laser irradiation), respectively. Measured temperature increments for heart tissue during 4W laser irradiation with 2-mm spot size are 12.89 °C, 3.38 °C for 3-mm and 5-mm deep from the surface (both of these thermocouple probes were placed on the direction of laser irradiation), respectively. Based on these findings, it can be stated that tissue temperature decreases exponentially as moving away from the target point of laser irradiation on the surface or as going deeper from the surface.

When tissue is irradiated with a laser beam, the fluence rate [W/m^2] of the beam inside the tissue decreases exponentially (Beer's law) [2]. The attenuation of the laser beam is due to absorption and possibly scattering of the collimated light according to the relation;

$$E(z) = (1-r_s) * E_0 * e^{-\mu t * z} \qquad (5.2)$$

Here,

E(z): the attenuated beam within the tissue [W/m^2]

E_0: the irradiance [W/m^2]

μ_t: the attenuation coefficient [1/m]

r_s : the Fresnel specular reflection for non-polarized light which is about 2% for light normal to an air-tissue interface.

As seen from the above equation, the local fluence rate decreases exponentially as moved away from the target point of laser irradiation. Because of the relation between temperature increment and local fluence rate (Eq. 5.2), by moving away from the target point of laser irradiation, temperature increment at tissue decrease exponentially. This situation was observed at the experimental results (3-mm and 5-mm deep measurements).

Beside the effects of distances from the target point of laser irradiation and laser output power levels on the measured temperature values, this study also illustrates some figures which compare the temperature increases for different tissue samples (lamb brain, heart and kidney). For 3-mm deep measurement, while there is a statistical difference between the temperature increments of brain and heart tissue at 2W and 3W laser output power values, there is no statistical difference between the temperature increments of brain and kidney tissues, and kidney and heart tissues. For example; for 2W laser output power level, measured temperature increments from the same thermocouple needle (TC-B) are 8.01 °C, 6.33 °C, and for 3W laser output power level, they are 12.95 °C, 9.44 °C for brain and heart tissues, respectively. For 5-mm deep measurement, while there is a statistical difference between the temperature increment of brain and heart tissues at 4W laser output power values, no statistical difference exists at 2W and 3W laser output power values. Also, there are no statistical differences between the temperature increments of heart and kidney tissues at all power levels (2W, 3W, 4W).

In photothermal interactions, absorption by water molecules plays a significant role. The absorption coefficient strongly depends on the wavelength of the incident laser radiation. In this study, 980-nm diode laser was used as the light source. This wavelength was selected because it is one of the peaks in the absorption spectra of water [7]. At some special wavelengths as in 980-nm, water content of the tissue mostly determines the thermal effect of tissue when it is irradiated by a laser light.

As stated above, three types of tissues (brain, heart and kidney) were used in this study. The water contents for these tissues are 77, 73.3, 72.4 percent for brain, heart and kidney respectively [22]. As a result of the experiments (3-mm and 5-mm deep measurements), it was observed that temperature increment for brain tissue is higher than heart tissue and there is no difference between the measured temperature values of heart and kidney tissues.

In conclusion, photothermal interactions of laser irradiation are being used at a large part of surgical and clinical applications. In these practices, the crucial thing is to know the temperature values at different radial and axial distances from the target point of tissue. In this study, different tissue samples (lamb brain, heart and kidney) were used and the

measured temperature increment for different distances and different laser output power values were compared. As a conclusion, it was observed that temperature increases are linearly positively correlated with the laser output power levels and, the distance from the target point of laser light has a negative exponential effect on the temperature increases.

In the future studies, experimental setup used in this thesis can be improved. Same procedure can be applied to other biological tissues with different laser output power levels and distances from the target point of laser irradiation. Also, the temperature distribution on different types of tissues related to distance and laser output power levels can be modeled. Therefore, it will be useful for clinical and surgical research where photothermal interaction of laser irradiation is being used.

REFERENCES

1. Gülsoy, M., "Biophotonics," BM516 lecture notes, Boğaziçi University, Istanbul, Turkey, unpublished, 2005.

2. Waynant, R.W., *Lasers in Medicine*, CRC Press, USA, 2002.

3. Niemz, M.H., *Laser-Tissue Interactions Fundamentals and Applications*, Springer-Verlag, Heidelberg, 1996.

4. Welch, A.J., "Laser physics and laser tissue interaction," *Texas Heart Institute Journal*, Vol. 16, pp. 141-149, 1989.

5. What is laser, http://www.hk-phy.org/articles/laser/laser_e.html

6. Laser Diodes, http://hyperphysics.phy-astr.gsu.edu/hbase/electronic/lasdio.html

7. Steele, R.V., "Diode-laser market grows at a slower rate," *Laser Focus World*, vol. 41, no. 2. 2005.

8. Manns, F., P.J. Milne, X.G. Cirre, D.B. Denham, J.M. Parel, and D.S. Robinson, "In situ temperature measurement with thermocouple probes during laser interstitial thermotheraphy," *Laser in Surgery and Medicine*, Vol. 23, pp. 94-103, 1998.

9. Tabakoğlu, H.Ö., "Effects of the 980-nm diode laser versus the monopolar electrocoagulator on the rat brain," Master's thesis, Bogazici University, Istanbul, Turkey, 2003.

10. Ishihara, M., T. Arai, S. Sato, Y.Morimoto, M. Obara, and M. Kikuchi, "Measurement of the surface temperature of the cornea during ArF excimer laser ablation by thermal radiometry with a 15- nanosecond time response," *Lasers in Surgery and Medicine*, Vol. 30, pp. 54-59, 2002.

11. Bartels, K.E., "Laser in Medicine and Surgery," *The Veterinary Clinics Small Animal Practice*, Vol. 32, pp. 495-512, 2002.

12. Manns, F., D. Borja, J.M. Parel, W. Smiddy, and W. Culbertson, "Semianalytical thermal model for subablative laser heating of homogeneous nonperfused biological tissue: application to laser thermokeratoplasty," *Journal of Biomedical Optics*, Vol. 8(2), pp. 288-297, 2003.

13. Lobik, L., A. Ravid, I. Nissenkorn, N. Kariv, J. Bernheim, and A. Katzir, "Bladder welding in rats using controlled temperature CO_2 laser system," *The journal of urology*, Vol. 99, pp. 1615-1662, 1999.

14. McNally, K.M., B.S. Sorg, A.J. Welch, J.M. Dawes, and E.R. Owen, "Photothermal effects of laser tissue soldering," *Phys. Med. Biol*, Vol. 44, pp. 983-1002, 1999.

15. Yang, W.J., and P.P.T. Yang, "Literature survey on biomedical applications of thermography," *Bio-Med.Mat. and Eng*., Vol. 2, pp. 7-18, 1992.

16. Gautherie, M., P. Haehenl, J.P. Walter, and L.G. Keith, "Long term assessment of breast cancer by liquid crystal thermal imaging," *Biomedical thermography*, pp. 279-301, New York, 1982.

17. Reid, A.D., M.R. Gertner, and M.D. Sherar, "Temperature measurement artifacts of thermocouples and fluoroptic probes during laser irradiation at 810 nm," *Physics in Medicine and Biology*, Vol. 46, pp. 149-157, 2001.

18. Bozkurt A, B. Onaral, "Safety assessment of near infrared light emitting diodes for diffuse optical measurements," *Biomedical Engineering Online*, Vol. 3(9), 2004.

19. Chin, L.C.L., W.M. Whelan, M.D. Sherar, and I.A. Vitkin, "Changes in relative light fluence measured during laser heating: implication for optical monitoring and modeling of interstitial laser photocoagulation," *Physics in medicine and biology*, Vol. 46, pp. 2407-2420, 2001.

20. Milne, P.J., J.M. Parel, and F. Manns, "Development of Stereotactically Guided Laser Interstitial Thermotherapy of Breast Cancer: In Situ Measurement and Analysis of the Temperature Field in Ex Vivo and In Vivo Adipose Tissue," *Lasers in Surgery and Medicine*, Vol. 26, pp. 67-75, 2000.

21. Liu, V.G., T.M. Cowan, and S.L. Jeong, "Selective photothermal interaction using an 805-nm diode laser and indocyanine green in gel phantom and breast tissue," *Lasers Med.Sci*, Vol. 17, pp. 272-279, 2002.

22. Cricuta, I.C., V. Simplaceanu, "Tissue water content and nuclear magnetic resonance in normal and tumor tissue," *Cancer Research*, Vol. 35, pp. 1164-1167, 1975.

23. Gülsoy, M., T. Celikel, A. Kurt, R. Canbeyli, I. Çilesiz, "980-nm wavelength diode laser application in stereotaxic laser neurosurgery in the rat," *Proc. SPIE*, Quebec, July, Vol. 3414, pp. 17-22, Canada, 1998.

24. Ivarson et all, "Feedback interstitial diode laser (805-nm) thermotherapy system:Ex vivo evaluation and mathematical modeling with one and four-fibers," *Laser in Surgery and Medicine*, Vol. 22, pp. 86-96, 1998.

25. Özer, K., "Optical properties of native and coagulated lamb brain tissues in vitro in the visible and near-infrared spectral range," Master's thesis, Boğaziçi University, Istanbul, Turkey, 2005.

26. Svaaand, L.O., and L.L. Randeberg, "Cooling efficiency of cryogen spray during laser therapy of skin," *Laser in Surgery and Medicine*, Vol. 32, pp. 137-142, 2003.

27. McDannold, N., K. Hynynen, and F. Jolesz, "MRI monitoring of the thermal ablation of tissue effects of long exposure times," *Journal of magnetic resonance imaging*, Vol. 13, pp. 421-427, 2001.

28. Şahin, B., "Effect of incident light intensity and source-detector separation on photon migration depth in turbid media," Master's thesis, Boğaziçi University, Istanbul, Turkey, 2006.

29. Duck, F.A., *Physical properties of tissue – a comprehensive reference book*, Academic Press, USA, 1990.

30. Sturesson, C., and S. Andersson, "A mathematical model for predicting the temperature distribution in laser-induced hyperthermia. Experimental evaluation and applications," *Phys. Med. Biol*, Vol. 40, pp. 2037-2052, 1995.

31. Özışık, M.N., *Boundary value problems of heat conduction*, International Textbook Company, Scranton, Pennsylvania, 1968.